Palaeoenvironmental evolution of late Miocene lacustrine deposits at Zahle (Bekaa Valley, Lebanon)

Josep Sanjuan[1*], Mohammad Alqudah[1, 2], Thomas A. Neubauer[3, 4], Jonathan Holmes[5], Catherina Khairallah[1]

[1]*Department of Geology, American University of Beirut, 11–0236 Beirut, Lebanon.*

[2] *Department of Earth and Environmental Sciences, Yarmouk University, 21163 Irbid, Jordan.*

[3] *Department of Animal Ecology and Systematics, Justus Liebig University, 35392 Giessen, Germany.*

[4] *Naturalis Biodiversity Centre, P.O. Box 9517, 2300 RA Leiden, The Netherlands*

[5] *Environmental Change Research Centre, Department of Geography, University College London, London WC1E 6BT, United Kingdom.*

*Corresponding author email address: js76@aub.edu.lb or josepst.juan@hotmail.com

Abstract

Neogene non-marine sedimentary rocks of the Bekaa Valley (Lebanon) are microfossil rich and show minimal lateral facies changes and post-depositional diagenetic alteration across continuous exposures. In this paper, we analyse the sedimentary facies and microfossils of three closely-spaced stratigraphic sections near the town of Zahle. The sedimentary sequence is divided, from base to top, into three intervals: (1) a massive conglomerate unit interpreted as

alluvial fan deposits, (2) fossiliferous yellowish marls and limestone interpreted as perennial lacustrine deposits, and (3) an organic-rich marlstone intercalated with volcanic ash horizons interpreted as a palustrine interval representing an overall shallowing sequence. Intervals 2 and 3 contain a diverse microfossil assemblage comprising charophytes, terrestrial molluscs, a freshwater bivalve, ostracods as well as fish and mammal remains. The palaeoenvironmental characteristics and evolution of these lacustrine deposits are inferred through facies analysis and through comparison of microfossil tolerances with the ecological requirements of their nearest living relatives. Results suggest that during the Miocene the Bekaa Valley was occupied by a relatively shallow, stable, oligotrophic freshwater or slightly oligohaline lake that evolved to a very shallow eutrophic lake with a dense palustrine vegetation belt. The palaeolake ultimately regressed to the south due to climatic changes and tectonic stresses leaving the lacustrine deposits exposed in the area of Zahle as an erosional surface.

Keywords: Neogene, lacustrine, Middle East, microfossil, sedimentology, palaeoecology.

1. Introduction

Neogene continental sedimentary rocks of Lebanon are well exposed in the Bekaa valley, especially in its eastern margin along paths and roads. These deposits show minimal post-depositional diagenetic alteration with lateral extension north-eastwards from the town of Zahle to the Chmistar village. In the area of Zahle, this sedimentary sequence displays a discontinuous vertical succession divided into three distinct intervals (Fig. 1).

The Neogene rocks of Zahle were first studied by Dubertret (1945, 1955) who identified and described the stratigraphic sequence. Dubertret (1945) defined this interval as a rock

sequence of conglomerates passing upwards into marl deposits rich in gastropods and intercalated with thin layers of lignite. Dubertret (1945) suggested a Messinian (latest Miocene) age for these deposits, yet without any palaeontological support. He used an imprecise lithostratigraphic correlation with similar stratigraphic sequences localised at the north of the same sedimentary basin. In agreement with Dubertret's suggestion, biostratigraphically relevant fossils from this lacustrine marl interval were first reported by Kansou (1961), who discovered a *Hipparion* horse tooth near the town of Zahle. A new fossil site with *Hipparion* teeth was discovered by Malez and Forsten (1989) in a southern locality near the village of Kefraya. Walley (1996) redefined these deposits in more detail naming them informally as the Zahle Formation. According to this author this rock unit is composed of three intervals with different lithologies; 1) thick deposits of conglomerates and breccia at the base passing upward to a 2) marl interval alternated with thin layers of limestone and lignite which is topped by 3) another interval of conglomerates. Little palaeontological work has been performed in the area during the last thirty years due to the Lebanese civil war and other international conflicts. A palaeontological analysis of rodent remains found in the area of Zahle has been recently performed by López-Antoñanzas et al. (2015). According to those authors the lacustrine deposits of Zahle, yielding the widely distributed taxon *Progonomys*, can be correlated with the European Mammal Neogene zones MN 10 or MN 11 (late Miocene, 9.9–7.6 Ma; Gradstein et al., 2012). However, a new micropalaeontological study based on charophytes from the same deposits suggests older ages (Sanjuan and Alqudah, 2018). Lateef (2003) assigned absolute ages of 10.4 ± 0.37 Ma and 10.87 ± 0.31 Ma (early late Miocene) to a basalt unit located northern and laterally and above the lacustrine deposits of Zahle, which is in agreement with recent biostratigraphic data based on rodents and charophytes.

In contrast to the amount of stratigraphic data available from these deposits, information about sedimentology, palaeoecology and palaeoclimate is scarce. In order to characterize the palaeoenvironmental conditions and the palaeoecological evolution of these non-marine deposits four field campaigns were performed from autumn 2016 to spring 2017 in the area of Zahle (Fig. 1). Three sections were studied in detail from the sedimentological viewpoint (facies analysis) and sampled systematically for microfossils. Hundreds of well-preserved fossils including molluscs, charophytes, ostracods and vertebrate remains were obtained from the studied sections. The large amount of well-preserved fossil remains and the good exposure of facies lay the basis for the palaeoecological reconstruction presented herein, shedding new light on the palaeoenvironmental characteristics of the lake, its sedimentological and limnological evolution, as well as the regional climatic conditions. This work also aims to create an inventory of Neogene microfossils of Zahle since the complete study area is under a high urbanization pressure threatening the outcrops and the fossil sites.

2. Geological setting

The Bekaa Valley represents a tectonic basin bounded by two anticline-systems representing the two mountain chains in Lebanon, i.e. the Mount Lebanon Mountain range in the west and the Anti-Lebanon Mountains in the East. The origin of the Bekaa Valley is related to tectonic folding and uplift of the aforementioned mountain ranges as a consequence of the collision between the joined African-Arabian and the Eurasian Plates during the Late Cretaceous (Lateef, 2007 and references herein). This tectonic phase is referred to as the Syrian Arc Event. While the mountain ranges formed subaerially exposed islands at that time, the synclines

represented epicontinental seas along the southern Neo-Tethys margin that accumulated thick marine sedimentary sequences (Alqudah et al., 2014). The Late Cretaceous to middle Eocene time was characterised by successive episodes of emergence and submergence due to alternating compressive and extensive movements, leading to variations in the sedimentation patterns across the Bekaa basin (Ponikarov, 1967; Lateef, 2007). During the early Palaeogene, parts of the anticlines emerged forming longitudinal islands oriented NE-SW. Palaeocene and lower/middle Eocene rocks are composed of chalky limestone beds and marls deposited in a shallow marine environment. During the late Eocene to Oligocene, the collision between the African-Arabian and Eurasian plates caused further uplift of the Lebanese geological structures and continental sedimentation commenced in the Bekaa Valley (Beydoun, 1999; Lateef, 2003). However, this regional uplift and the continentalization of the valley have never been dated precisely.

Biostratigraphic studies based on nannofossils suggest that the first inversion and elevation of northern Mount Lebanon occurred between latest Maastrichtian to Early Paleocene time (C. Müller et al., 2010). These authors dated a second elevation phase during the pre-Early Miocene.

This second tectonic phase resulted in a flexural subsidence in the northern part of the Middle East leading to a major progradation of the marine facies (Alsharhan and Nairn, 1997). As a consequence of high tectonic activity, the intense erosion of the uplifted areas resulted in high rates of synorogenic deposition (mainly conglomerates related to alluvial fan deposits) within the Bekaa Basin and other Levantine basins during the early Miocene (Lateef, 2007).

The Dead Sea transform fault formed probably in the middle to late Miocene favouring the development of extensive volcanism in the region, further uplift of the Lebanon and Anti-

Lebanon Mountains and deepening of the proto-Bekaa Valley (Ponikarov, 1967). Macro-geomorphic features studied by Gomez et al. (2006) suggest that this uplift phase was asymmetric between the Mt. Lebanon and Anti Lebanon ranges. This tectonic event increased the accommodation space infilled by more synorogenic alluvial and lacustrine deposits. Lacustrine systems occupying large parts of the basin became the dominant sedimentary environments during the middle to late Miocene. Younger uplift and tilting occurred during the Pliocene and Quaternary in the Syrian Coastal Range and some areas of Lebanon (Gomez et al., 2006).

3. Materials and Methods

Fossil remains were recovered from three stratigraphic sections closely related that can be correlated in the field, covering the lower, middle and upper parts of the Neogene deposits of Zahle (Figs. 1 and 2). The section 1 is located at the lower part of the lacustrine sequence (base of the section: 33º51'22.2"N, 35º53'39"E, top of the section: 33º51'15.12"N, 35º53'49"E). The overlying section 2 is situated about 250 m westwards to the previous section (base of the section: 33º51'14.69"N, 35º53'55.65"E, top of the section: 33º51'13.1"N, 35º53'55.69"E). The upper section 3 follows a path located about 500 m westward of the previous section (base of the section: 33º51'05.95"N, 35º54'14.95"E, top of the section: 33º51'02.77"N, 35º54'22.96"E).

Microfossils were obtained from twelve samples (Z-0 to Z-11) of grey/yellowish lacustrine marls collected from the aforementioned sections (Fig. 2). About 2 kg of sediment per sample were disaggregated in solution composed of water, hydrogen peroxide and Na_2CO_3 and later sieved using sieves with five different mesh sizes, i.e. 1.0 cm, 0.85, 0.65, 0.35 and 0.25 mm.

Microfossils were picked out under a light microscope. The relative amount of microfossils picked out from the samples is based on a semi-quantitative visual estimation (Table 1). Selected fossils were photographed and studied using a scanning electronic microscope MIRA 3LMU at the Central Research Science Laboratory of the American University of Beirut and at the Department of Earth Sciences, University College London. Thin-sections, about 30 μm in thickness, were prepared from rock samples from selected limestone beds in order to describe the microfacies. The material here studied and illustrated is housed in the Geology Museum of the American University of Beirut (acronym AUBGM).

----------Figure 2 near here----------

4. Depositional Environments

The studied sections overlie an Eocene nummulitic limestone bed dipping 50º East. The Neogene deposits dip 30º East and can be divided into three basic types of facies assemblages: 1) alluvial fan clastic facies deposits, 2) perennial lake marl and limestone beds, and 3) palustrine organic-rich marls.

4.1. Alluvial fan clastic deposits

Clastic deposits are located at the base of section 1. This interval is about 30 m thick and consists of massive clast-supported oligomict conglomerates (Figs. 3C and 4). Deposits are poorly sorted and lack sedimentary structures. Clasts are subrounded in shape and variable in size ranging between 5 to 40 cm in diameter. All clasts are composed of nummulitic limestone suggesting that the clasts' source rock is the underlying Eocene nummulitic limestone.

155 Conglomerates become less massive at the top of the section showing more concentrated clasts
156 and becoming alternated with metre-scale silty intervals rich in ostracods (Fig. 3C).

157 The massive and structureless conglomerates located at the base of section 1 are related
158 to debris flow deposits in an alluvial fan context (Boggs, 2011). The increase of clast
159 concentration at the upper part of the interval together with the presence of silt suggests a
160 progressive change from debris to stream flow sedimentary processes. Moreover, the presence of
161 ostracods in silty deposits indicates that sedimentary processes occurred in a subaquatic context.
162 The abundant supply of sediment in the area is a consequence of high tectonic activity, i.e. fault
163 displacement, during the first stages of the lacustrine system.

164 *4.2. Lacustrine marl and limestone beds*

165 This soft rock interval comprises the upper part of section 1, the complete section 2 and
166 base of section 3. In general marls and sandy marls are arranged forming monotonous beds,
167 metre-scale in thickness, light grey to yellowish in colour and alternated with limestone and few
168 lignite layers (Fig. 3D-E and Fig. 4). These deposits are very rich in fossil remains of gastropods,
169 charophytes and ostracods. Small gastropods of the family Hydrobiidae are especially abundant
170 in most of the intervals, representing by far the dominant fossils of the three stratigraphic
171 sections (Fig. 3E, Table 1).

172 Several cycles of a characteristic facies succession formed by marls at the base passing
173 upwards to silts and topped with limestone can be observed in the sections 1, 2 and base of
174 section 3. Marls are organised in grey to yellowish sets of beds ranging in thickness from 0.3 to 1
175 m. They show diffuse lamination and contain abundant and well-preserved fossil remains,

mainly gastropods and charophytes. Silty marls contain a few organic-rich dark-grey horizons which are 5–10 cm thick showing poorly preserved comminute plant debris. No edaphic features have been observed underlying these layers in section 1. Limestone layers are represented by low-cemented wackestone–packstone, generally light grey in colour and forming irregularly tabular beds of 20–50 cm in thickness. The most common components of these limestone intervals are gastropods shells, frequently dissolved and forming a secondary moldic porosity (Fig. 3A–B). Microfossil content is very diverse composed of gastropods, charophytes, ostracods, bivalves, fish otoliths and vertebrate remains. Freshwater gastropods belonging to Hydrobiidae family are especially abundant along with the ostracod *Cyprideis* sp.

---------- Figure 3 near here ----------

The vertical succession of facies changing from monotonous fossiliferous marls with some lignite horizons grading upwards to wackestone–packstone limestone intervals can be interpreted as the increasing abundance of calcareous organisms in the shallower and well-illuminated lacustrine environments. The marls were probably deposited in more distal and deeper lacustrine facies than the limestones. Despite the high content of fossils in the marl interval, the facies show some intervals of diffuse lamination and they contain a few lignite horizons with comminute plant fragments suggesting that the lake bottom was occasionally anoxic, hindering bioturbation and preserving the plant remains (Gierlowski-Kordesch, 2010). Moreover, no edaphic features have been observed underlying these lignite horizons indicating that plant remains were probably transported from the lakeshore and sank in the deeper areas forming an allochthonous assemblage on the lake bottom. Microfossils are well-preserved and do

not show signs of fragmentation suggesting that fossils were buried *in situ* or after minor transport, although the lack of juvenile ostracod valves in sample Z-6 suggests that higher-energy conditions, which led to the winnowing of the smaller and lighter juvenile valves, must have prevailed during at least some of the interval represented by the sediment record. Fossils occur in both marls and limestones and from the sedimentological viewpoint they correspond to biogenic carbonate producers. The presence of charophyte gyrogonites and thalli suggest that the lake bottom was well-oxygenated and well-illuminated. Dissolved gastropod shells are related to secondary diagenetic processes. The absence of ripples and broken shells in almost all sections 1 and 2 suggests that the depositional environment was relatively quiet, without the action of strong waves or currents. The presence of limestone layers indicates a change of the environmental conditions. The predominance of wackestone and packstone fabrics indicates moderate energy sedimentation (Boggs, 2011).

4.3. Palustrine organic-rich marls

These deposits are mainly located at the upper part of section 3 (Fig. 4). Marls and marly siltstones are organised in yellowish or dark grey beds ranging in thickness from 0.3 to 0.5 m. These deposits are mostly made of tabular beds, sometimes with erosive bases (Fig. 3F). They contain abundant organic matter rich marl intervals forming lignite of 5–10 cm in thickness, some volcanic ash intervals, burrowing structures, root traces and a high diversity of fossils, mainly gastropods (Fig. 3G). This palustrine facies could be classified in the type facies number 7 (organic-rich marlstone and clays) described by Alonso-Zarza (2003) and Alonso-Zarza and Wright (2010). Large numbers of the mollusc shells do not occur in life position, although well-preserved specimens are concentrated in some intervals. Large broken gastropod shells mostly

220 belong to the species *Melanopsis buccinoidea*, which occasionally forms accumulations of about
221 5–10 cm thickness (Fig. 3H).

222 Dark-grey coloured marls and silty marl intervals with abundant lignite horizons suggest
223 a higher concentration of organic matter (plant remains) deposited in locally anoxic conditions.
224 The presence of edaphic structures, which are particularly abundant below the lignite horizons,
225 indicate that plant remains were not transported (autochthonous taphoflora) and the plant
226 community grew *in situ* in the lake shores forming occasionally peat swamps (Gastaldo et al.,
227 1995). Sedimentological characteristics suggest that sediments of section 3 were deposited under
228 extremely shallow lake conditions at the lake margin where halophytic plants grew forming local
229 peat swamps. Small fossils are well-preserved, while large gastropod shells are fragmented and
230 occasionally form coquinas. This evidence suggests that shells were exposed to an energetic
231 environment, probably subjected to wave activity at the lake shore or re-working episodes due to
232 water level fluctuation and/or periodic exposures. The abundance of ash intervals in this section
233 may indicate an increase of the volcanic activity in the area.

234 ---------- Figure 4 near here ----------

235

236 **5. Micropalaeontology**

237 *5.1. Characeae*

238 Charophytes represent a group of aquatic plants living in freshwater or brackish water
239 conditions (Krause, 1997). Their biomineralised fructifications (gyrogonites and utricles)
240 frequently fossilize and have been traditionally used as biostratigraphic markers of non-marine

241 deposits (Soulié-Märsche, 1989). The usefulness of charophytes lies in their sensitivity to
242 palaeoenvironmental change and specific habitat requirements (Gierlowski-Kordesch, 2010).
243 Hence, fossil charophytes have been used as a palaeoecological proxies specially in Neogene and
244 Holocene non-marine deposits providing valuable information about palaeosalinities, water level
245 fluctuation and changes in trophic status (García and Chivas, 2006; Martín-Closas et al., 2006;
246 Soulié-Märsche et al., 2010; Sanjuan and Alqudah, 2018). Recent studies involving experimental
247 cultures have been developed with the aim to use geochemistry (trace-elements and oxygen
248 isotopes) to reconstruct palaeosalinities and palaeotemperatures (Dux et al., 2015) and to find
249 links between gyrogonite morphology and ecological parameters such as temperature and light
250 irradiance (Sanjuan et al., 2017). Moreover, species-specific palaeoenvironmental constraints
251 have been defined for Mesozoic and Cenozoic fossil charophytes based on sedimentological and
252 taphonomical analyses (Villalba-Breva and Martín-Closas, 2011; Sanjuan and Martín-Closas,
253 2012; Vicente et al., 2016).

254 Charophyte gyrogonites belonging to five taxa have been recognised in the lacustrine
255 deposits of Zahle, i.e. *Nitellopsis* (*Tectochara*) *merianii*, *Lychnothamnus barbatus* var. *antiquus*,
256 *Chara microcera*, *Chara* cf. *globularis* and *Sphaerochara* sp. Three of these taxa have been
257 recently described and illustrated by Sanjuan and Alqudah (2018).

258 *Nitellopsis* (*Tectochara*) *merianii* (Grambast and Grambast-Fessard, 1954) Grambast and
259 Soulié Märsche, 1972 occurs abundantly and well preserved in three samples from section 1 and
260 one sample from section 2 (Fig. 5, Table 1). This fossil species is considered the ancestor of the
261 living species *Nitellopsis obtusa* (Desv. in Loisel.) Groves (Soulié-Märsche et al., 2002; Sanjuan
262 and Martín-Closas, 2015). These authors linked both species to an evolutionary lineage that

263 ranges from the latest Eocene (late Priabonian) to the Quaternary. *N. obtusa* is a boreal species
264 that is exclusively distributed in deep and shallow large, cold lakes of northern Europe, Asia and
265 North America (Corillion, 1972; Soulié-Märsche et al., 2002). In these permanent lacustrine
266 habitats *N. obtusa* forms large and dense meadows of up to 2 m height covering the lake ground.
267 It thrives in oligotrophic/mesotrophic alkaline waters in depths over 4 m (Krause, 1985; Soulié-
268 Märsche et al., 2002). Gyrogonites of *Lychnothamnus barbatus* var. *antiquus* Soulié-Märsche,
269 1989 occur in three samples of section 1 (Fig. 5, Table 1). The typical depth range of the living
270 species *Lychnothamnus barbatus* in Europe is from 2 to 8 m where it forms dense meadows of
271 up to 1 m high plants (Krause, 1985). This species has been traditionally related to cold and
272 oligotrophic freshwaters usually associated to phreatic origin from northern Europe (Krause,
273 1997; Soulié-Märsche and Martín-Closas, 2003). However, recent studies performed in central-
274 western Poland concluded that *L. barbatus* can also thrive under eutrophic conditions (Pelechaty
275 et al., 2017). Specimens of *Chara* cf. *microcera* Grambast and Paul, 1965 have been extracted
276 from two samples at the base of section 1 (Fig. 3, Table 1). Although there is no living
277 representative of this species, previous micropalaeontological studies suggested that this extinct
278 species grew in perennial freshwater lakes (Sanjuan et al., 2014). Many specimens of *Chara* cf.
279 *globularis* Thuiller, 1799 have been recovered from a large number of samples through the
280 sections. It appears abundantly at the top of section 3, especially in samples Z-10 and Z-11 (Fig.
281 5, Table 1). *Chara globularis* lives in permanent or temporary shallow bodies of water. This
282 species has a strong tolerance to eutrophication and is able to survive in areas with low light
283 irradiance and very cold water temperatures, even resistant to lakes with frozen surfaces (Bailly
284 and Shaefer, 2010). Few gyrogonites of *Sphaerochara* sp. occur in sample Z-10 (Fig. 5, Table 1).
285 Gyrogonites are medium in size, 630 μm high and 533 μm wide (mean values), spheroidal in

shape showing nine convolutions in lateral view displaying a characteristic ornamentation formed by large and regularly spaced tubercles arranged along the spiral cells (Fig. 5O–Q). No ecological requirements can be deduced for this species since it does not have extant representatives. Corticated charophyte stems (thalli) belonging to genus *Charaxis* sp. appear in many samples suggesting that charophyte meadows were growing in situ (Table 1).

----------Figure 5 near here----------

5.2. Molluscs

Non-marine molluscs are widely used as palaeoenvironmental indicators (e.g. Ložek, 1964; Goodfriend, 1992; Ciangherotti et al., 2007; Salvador et al., 2016; Neubauer et al., 2017; Harzhauser and Neubauer, 2018). Many extant relatives of species found in the fossil record are typical of very specific ecological conditions (e.g. Glöer, 2002; Welter-Schultes, 2012).

Nine freshwater gastropod species have been recovered from the studied stratigraphic sections. Many well-preserved shells of *Valvata saulcyi* Bourguignat, 1853 have been picked out from marls in section 3 (Fig. 6A–C, Table 1). This living species thrives in slowly running headwaters of rivers, ponds, springs, channels and lakes on muddy-sandy bottoms to hard grounds, as well as in ditches with stagnant water, preferably with aquatic vegetation. The species is tolerant of (slight) salinity increases and eutrophication (Germain, 1921; Yıldırım, 1999; Şereflişan et al., 2009; Bößneck, 2011; Van Damme and Kebapçı, 2014). A large number of opercula belonging to *Bithynia* sp. have been extracted from many samples throughout the

sections (Fig. 6D–E, Table 1). Species of this genus dwell in moving and standing water bodies, also in temporarily drying water bodies, on muddy bottoms, rock or plants (Welter-Schultes, 2012). Shells of *Melanopsis buccinoidea* Olivier, 1801 have been recovered from three samples from sections 2 and 3 (Fig. 6F, Table 1). Adult specimens can attain 5 cm in height, and they have been spotted also in some intervals at the top of section 3 (Fig. 3H). This species, nowadays native to the Middle East, dwells in various freshwater habitats, including streams, ponds, springs, pools and swamps (Van Damme, 2014).

Three species of mud snails (Hydrobiidae) have been recovered from the three studied sections. *Semisalsa* sp. is abundant in many samples (Fig. 6G–H, Table 1). This genus has a broad ecological amplitude occurring in brackish water environments, estuaries, salt lakes and non-tidal lagoons, coastal rivers, as well as in freshwater springs, wells, ponds and lakes (Bank and Butot, 1984; Glöer, 2002). Many specimens of *Pseudamnicola* sp. have been recovered abundantly in all the samples from section 1 (Fig. 6I, Table 1). Species of *Pseudamnicola* dwell in coastal streams, lakes, ponds, low river courses, springs and thermal springs (Szarowska, 2006; Glöer et al., 2010; Delicado et al., 2015). Hundreds of shells of *Islamia* sp. have been picked out from almost all the samples studied being the most abundant microfossil recovered (Fig. 6J–K, Table 1). Living species of *Islamia* are found in subterranean waters and springs, occasionally also in rivers and lakes (Bodon et al., 2001; Arconada and Ramos, 2006; Radea et al., 2017).

Few specimens of *Radix* sp. have been recovered from samples Z-10 and Z-11 (Fig. 6L, Table 1). Species of the genus *Radix* are found in standing or slowly moving waters often rich in vegetation (Welter-Schultes, 2012).

329 Two species of Planorbidae have been obtained from the three studied sections. *Gyraulus*
330 cf. *piscinarum* Bourguignat, 1852 occurs in low numbers in all the sections becoming more
331 abundant at the top of section 3 (samples Z-7 and Z-9) (Fig. 6N–O, Table 1). This species dwells
332 in swamps and slowly flowing, vegetated waters (Heller, 2009). Few specimens of *Gyraulus* cf.
333 *hebraicus* Bourguignat, 1852 has been recovered from three samples (Fig. 6M, Table 1). Seddon
334 (2014) suggests that this species thrives in ponds and vegetated rivers.

335 Three species of terrestrial microgastropods have been extracted from section 3. A
336 relatively large number of *Carychium* sp. shells occur in samples Z-8, Z-9 and Z-11 (Fig. 6P,
337 Table 1). Living *Carychium* species require humid or wet conditions and are found in forests,
338 meadows and swamps among leaf litter, under decaying wood and between stones (Welter-
339 Schultes, 2012). Few specimens of *Vertigo* cf. *antivertigo* Draparnaud, 1801 have been picked
340 out from samples Z-8, Z-10 and Z-11 (Fig. 6Q, Table 1). This hygrophilous species dwells in
341 swampy meadows, along river and lake margins and in regularly flooded areas, mainly among
342 rotting plant material. This species needs permanent moist habitats and it cannot thrive in places
343 subjected to temporary droughts (Welter-Schultes, 2012). *Vertigo* is at present a widespread
344 genus of humid habitats or regions, chiefly in the Northern Hemisphere. Members of *Vertigo*
345 occur both in subarctic woodland of Norway and, much more rarely, in American tropics
346 (Stworzewicz, 2009). Few shells of *Strobilops* sp. occur in sample Z-11 (Fig. 6R, Table 1).
347 Extant species of *Strobilops* live in decaying logs and dead leaves in moderately humid forests
348 (Pilsbry, 1927). No record of this genus has been found after the Pliocene in Europe since it
349 became extinct in Europe before the first major glaciation.

350 ----------Figure 6 near here----------

One species of bivalves of the family Sphaeriidae, *Pisidium* cf. *moitessierianum* Paladilhe, 1866, has been extracted from samples Z-5, Z-6, Z-8 and Z-9 (Fig. 6S–U, Table 1). This species requires slowly moving, well-oxygenated hard water over clean, unpolluted substrates varying from fine mud to sand. It dwells in lowland rivers, canals and large lakes with moderately moving water (Welter-Schultes, 2012).

----------Table 1 near here----------

5.3. Ostracods

Ostracods are small aquatic crustaceans that secrete bivalved shells made of low-Mg calcite. They are common in most types of water of circum-neutral to alkaline pH and their shells are often abundant and well preserved in Neogene sediments (e.g. Anadón et al., 2002; Rodriguez-Lazaro and Ruiz-Muõz, 2012). Non-marine ostracods are sensitive to a range of environmental variables, including the size, depth and energy level of the waterbody, hydrochemistry, water temperature, dissolved oxygen concentration, trophic status and predation (Mesquita-Joanes et al., 2012) and they have excellent potential as palaeoenvironmental indicators (Anadón et al., 2002). Some species also display well-characterized ecophenotypic responses to environmental variations, especially hydrochemistry and variations in size and morphology may thus provide complementary palaeoenvironmental information (Boomer et al., 2003). Ostracods grow by moulting, up to eight times prior to adulthood. Because the different moult stages have contrasting hydrodynamic properties, the size distribution of moults within a stratigraphic interval can indicate whether a fossil assemblage has been subjected to post-mortem reworking by current action (Whatley, 1983; De Deckker, 2002). Adult ostracod carapaces often disarticulate into the constituent valves following death. Although different species show

373 variable tendency to such disarticulation, the presence of large numbers of articulated carapaces
374 within a fossil assemblages suggests low-energy conditions at the time of deposition and/or high
375 rates of sediment accumulation and hence rapid burial (De Deckker, 2002).

376 Four ostracod species have been recovered from the studied sections, which are, in order
377 of decreasing abundance, *Cyprideis* sp., *Cypris pubera* O.F. Müller, 1776, *Candona* cf. *angulata*
378 G.W. Müller, 1900 and *Strandesia* sp.

379 Large numbers of *Cyprideis* sp. occur in samples Z-5, 6, 7 and 8 (Fig. 7A-N, Table 1). In
380 samples Z-5, 7 and 8, adults and juvenile moults were recovered, whereas in Z-6, juvenile moult
381 stages were rare. Valves and carapaces were common in all samples. A few individuals display
382 moderately prominent nodes, but most are un-noded. The specimens from Zahle closely
383 resemble the widespread and well-known species *Cyprideis torosa* (Jones, 1850). This species
384 evolved in the Neogene or early Pleistocene and is at present common in marginal marine and
385 athalassic saline waters (Gliozzi et al., 2017). It is extremely euryhaline, tolerating a wide range
386 of salinities from around 0.5 to 60 psu or more, although its optimum ranges appears to be in
387 more dilute waters, from about 17 to 20 psu (Wouters, 2017). In athalassic environments, it is
388 generally restricted to waters with an alkalinity to calcium ratio less than unity, i.e. waters whose
389 anion composition is dominated by chloride or sulphate (De Deckker and Lord, 2017). The
390 species is generally found in shallow waters, <10 m deep (Pint et al., 2012), and is tolerant of a
391 wide range of dissolved oxygen concentrations, with the ability to tolerate dysaerobic conditions
392 (Pint and Frenzel, 2016). The species is able to tolerate water temperatures from at least 5 to
393 20°C, although it is more productive at higher end of this range (Ruiz et al., 2013) and requires a
394 temperature of at least 14 to 15˚C for the eggs to hatch (Heip, 1976; Frenzel et al., 2012).

Cyprideis torosa shows strong salinity-driven ecophenotypic response in valve size (Boomer et al., 2017), noding (Frenzel et al., 2012) and sieve pore morphology (Frenzel et al., 2017); variations in these characteristics in fossil shells have been used for palaeosalinity reconstructions (De Deckker and Lord, 2017). Preliminary morphological observations of specimens from the Zahle sequence are consistent with salinity values greater than about 8.5 to 9.5 psu based on lengths of adult female left valves (0.95 ± 0.04 mm, n = 31: cf. Fig. 5 in Boomer et al., 2017) and about 8 to 9 psu based on the predominance of non-noded valves. However, these interpretations derive mainly from works on *C. torosa* in a marginal marine context (Van Harten, 2000; Keyser, 2005; Frenzel et al., 2012). Athalassic lakes may have contrasting ionic composition to marginal-marine environments, in which the relationship between shell morphology and salinity differs (Boomer et al., 2017).

Firm identification of Miocene *Cyprideis* is problematical because of the close similarity in valve features of *C. torosa* to several other proposed species, all of which are now extinct. These are *C. agregentina* Decima, 1964*, C. ruggierii* Decima, 1964 and *C. crotonensis* Decima, 1964; together with *C. torosa,* they make up the *Cyprideis torosa*-group. Whether these represent truly distinct species or are simply a manifestation of intraspecific variability within *C. torosa* remains unresolved (Ligios and Gliozzi, 2012; Gliozzi et al., 2017). Based on comparison of a few specimens with the detailed morphological descriptions in Gliozzi et al. (2017), the Zahle material shows similarity with *C. ruggierii* (Elsa Gliozzi, pers. comm. 2018). However, determinations of more specimens from Zahle are needed to confirm this and, for the moment, the species is left in open nomenclature.

Most important for paleoenvironmental reconstruction is whether the ecophenotypical responses developed for living *Cyprideis torosa*, especially the quantitative morphological transfer functions based on valve size, sieve pore morphology and degree of noding, can be applied to Neogene material such as that from Zahle. Grossi et al. (2015) have shown that adult valve size and sieve pore morphology of Messinian *C. agrigentina* appear unrelated to salinity inferred from palaeoecology and geochemistry, whereas the convergence of our results based on valve size and noding, suggest that the relationships described for *C. torosa* may hold for the species found in the Zahle sequence. However, given the uncertainties about the identification of the material from Zahle, and the ionic composition of the palaeo-lake, the paleoenvironmental significance of *Cyprideis* morphology should be treated with caution pending further investigations.

Cypris pubera (Fig. 7O) is a minor component of three samples, present as adult and juveniles shells, although there are too few specimens to comment conclusively on the ontogeny. *Cypris pubera* is widely distributed across Europe and the Middle East, and most commonly found in shallow water; it can tolerate elevated salinity up to about 4 psu and is described as mesothermophilic (Meisch, 2000), associated with July and January air-temperature ranges of 8 to 28˚C and -31 to 14˚C, respectively (Horne et al., 2012).

Candona cf. *angulata* (Fig. 7Q) is present in small numbers in Z-5. The adult valve resembles *C. angulata* in outline, but too few specimens were recovered to be certain about the identification or to comment on the ontogeny: the juvenile candonids in this sample are assumed to belong to the same species as the adult specimen. *Candona angulata* prefers brackish water and is often found in coastal lakes with some input of seawater. It is found in waters with salinity

438 from 0.2 to 14 psu and often co-occurs with *Cyprideis torosa* which is mesothermophilic
439 (Meisch, 2000), and associated with July and January air-temperature ranges of 16 to 25˚C and -
440 5 to 17˚C, respectively (Horne et al., 2012).

441 *Strandesia* sp. (Fig. 7P) is represented by a single specimen in sample Z-1. The specimen
442 clearly belongs to the group of species of *Strandesia* that display protuberances on the dorsal
443 margin of the right valve: however, this specimen could not be identified to species level.

444

445 ---------- Figure 7 near here ----------

446

447 *5.4. Other microfossils*

448 Other biogenic structures such as an indeterminate bone fragments, a crocodile tooth, few
449 rodent teeth related to the extinct genus *Progonomys* (pers. comm. Isaac Casanovas and Raquel
450 López-Antoñanzas), fish otoliths related to the Cichlidae and Gobiidae families (pers. comm.
451 Werner Schwarzhans) and many fish teeth have been extracted from the studied sections (Table
452 1).

453

454 **6. Discussion**

455 *6.1. Microfossil taphonomy and palaeoecology*

456 The lacustrine deposits from Zahle yielded a large and diverse number of microfossils
457 (charophytes, molluscs, ostracods and vertebrate remains) that display a characteristic vertical
458 succession and facies association, providing valuable information for the understanding of the
459 palaeoenvironmental evolution of the palaeolake through time. In general, two microfossil
460 assemblages can be distinguished in agreement with the facies succession, i.e. one assemblage
461 from lacustrine marls (top of the section 1, section 2 and base of the section 3) and one from the
462 palustrine marls (upper part of section 3).

463 Seven species of aquatic gastropods have been recognised in marls from these three
464 sections. Three hydrobiid species (*Semisalsa* sp., *Islamia* sp., and *Pseudamnicola* sp.) represent
465 the dominant fossils in these deposits, accompanied by *Gyraulus* cf. *piscinarum*, *Gyraulus* cf.
466 *hebraicus*, *Valvata saulcyi* and *Bithynia* sp. (Table 1). Living representatives of *Semisalsa* and
467 *Pseudamnicola* have broad ecological requirements and live in brackish or freshwater water
468 environments (estuaries, rivers, springs, ponds and lakes). Similarly, species of *Islamia* are found
469 in a wide array of habitats, ranging from subterranean waters and springs to lakes and rivers. The
470 presence of the freshwater bivalve *Pisidium moitessierianum* suggests that well oxygenated,
471 calm and alkaline waters conditions prevailed in the palaeolake. The charophyte assemblage in
472 these deposits is dominated by the species *Nitellopsis* (*Tectochara*) *merianii* which appears
473 abundantly in samples from the section 1 (Table 1). Other species appear less abundantly also in
474 sections 1, 2 and base of the 3 i.e. *Lychnothamnus barbatus*, *Chara microcera* and *Chara* cf.
475 *globularis* (Table 1). The occurrence of the fossil species *Nitellopsis* (*Tectochara*) *merianii* and
476 *Lychnothamnus barbatus* var. *antiquus* is significant from the palaeolimnological viewpoint. The
477 two taxa represent the ancestors of the extant boreal species *Nitellopsis obtusa* and
478 *Lychnothamnus barbatus*, respectively. The predominance of *Nitellopsis* (*T.*) *merianii* suggests

479 permanent and relatively deep (2–8 m deep), oligotrophic lake conditions (fig. 8). The ostracod
480 assemblage is dominated by *Cyprideis* sp., which is especially abundant in section 2.
481 Notwithstanding uncertainties about the identification of this ostracod species, the ostracod
482 assemblage may suggest moderate-depth (<10 m), possibly dysaerobic and oligohaline water
483 with a low alkalinity/Ca ratio, but with the strong caveat that these inferences, which are based
484 on living *Cyprideis torosa*, may not apply to the Miocene-age material. The rise in the number of
485 *Cyprideis* sp. carapaces in the second section may suggest an increase in lake salinity reflecting
486 either in response to more arid conditions or as a result of a hydrographic change from an open to
487 a closed lake system. Mollusc shells are well preserved, showing only few signs of abrasion.
488 Charophytes gyrogonites show their original mineralogical constituents (endocalcine and
489 ectocalcine), without any trace of dissolution or corrosion occurring in association with
490 fragments of charophyte stems (thalli). This evidence suggests that the fossil assemblages from
491 sections 1 and 2 were buried *in situ* or after short-distance transport.

492 The sedimentological, micropalaeontological and taphonomic analyses suggest that marls
493 and limestones were deposited in a permanent fresh or oligohaline, relatively shallow,
494 oligotrophic and alkaline lake with a soft muddy bottom.

495 A dramatic change of the microfossil content can be observed in the upper art of section
496 3. Terrestrial microgastropod shells of *Carychium* and *Vertigo* are relatively abundant. In
497 addition, the gastropods *Semisalsa* and *Pseudamnicola* disappear in this interval while other
498 aquatic groups related to stagnant conditions and vegetated waters (*Valvata, Radix* and
499 *Gyraulus*) appear or increase in number (Table 1). Similarly, charophyte species related to
500 perennial-deep and oligotrophic lacustrine conditions present in sections 1 and 2 such as *N.* (*T.*)

501 *merianii* and *L. barbatus* are absent in this palustrine interval. On the other hand, *Chara* cf.
502 *globularis*, which has a wide ecological amplitude, shows a considerable increase. No ostracod
503 carapaces have been found in the upper part of section 3. Although this may imply that
504 conditions were unfavourable to ostracods at this time, this seems surprising given the abundance
505 of remains of other aquatic fauna, suggesting instead that it may be the result of taphonomic
506 effects.

507 ---------- Figure 8 near here ----------

508 Shells of large gastropods appear fragmented especially in the uppermost part of the
509 section, and some specimens of terrestrial gastropods show signs of abrasion (Fig. 6Q). In
510 contrast, no signs of dissolution or abrasion have been observed in gyrogonites of *Chara* cf.
511 *globularis*. Hence, while charophytes and some gastropod species (*Islamia, Valvata, Radix* and
512 *Gyraulus*) thrived *in situ*, larger aquatic and terrestrial gastropods were transported.

513 The sedimentological, micropalaeontological and taphonomic analyses indicate that rocks
514 at the top of section 3 were deposited in very shallow, eutrophic conditions at a vegetated lake
515 margin. The presence of broken shells intervals forming coquinas suggests that the lake margin
516 was subjected to current or wave activity or subaerial exposure related to water level fluctuations
517 (fig. 8).

518 *6.2. Tectonic implications*

519 Tectonic activity represents, along with the climate, a key parameter controlling the lake
520 topography, hydrology (open/closed), the mechanisms of water supply and the sources of
521 chemical constituents affecting the water chemistry (Alonso-Zarza and Wright, 2010).

522 The position of the lake and its morphology was controlled by the location and rates of
523 movement of the Yammouneh fault located about 3 km westward in the same area (north
524 extension of the Dead Sea transform fault). The vertical change of facies described here may
525 respond to tectonic pulses of the fault during the Miocene. Clastic alluvial fan deposits located at
526 the base of section 1 clearly indicates a period of erosion and transport due to the very high
527 tectonic activity. The sedimentological characteristics of the overlying carbonate deposits, i.e.
528 marls and limestone related to perennial-lake conditions, suggest that the tectonic activity
529 decreased. A fossil charophyte assemblage recovered from the base of these lacustrine deposits
530 containing biostratigraphically relevant taxa suggest that the establishment of the palaeolake took
531 place during the early-middle Miocene (Sanjuan and Alqudah, 2018). The presence of palustrine
532 marls and organic-rich clays in section 3 may indicate that the fault remained inactive in the
533 region during the last stage of the palaeolake sequence.

534 *6.3. Palaeoclimate implications*

535 Little is known about the climatic and palaeoenvironmental evolution of Lebanon during
536 the Miocene. The fossil assemblage recovered from lacustrine deposits of Zahle may shed light
537 on the palaeoclimatic setting of the Bekaa Valley and the Eastern Mediterranean region during
538 the late Miocene. However, the palaeoecological evidence presented here suggests
539 reconstructions based on the various fossil groups are, to some degree, contradictory.

540 Several of the fossil taxa recovered from the Zahle sequence provide information about
541 past temperatures. The two charophyte species recorded in section 1, i.e. *N.* (*T.*) *merianii-obtusa*
542 and *Lychnothamnus barbatus*, are considered boreal taxa growing mainly in north European
543 cold-water lakes (Corillion, 1972). The dominant species *N. merianii-obtusa* grows in permanent

544 lakes with an average summer water temperature of 16 Cº (Larkin et al., 2018). This seems
545 surprising, however, given the widespread evidence that the late Miocene, although cooler than
546 the earlier part of the Miocene, was warmer than present. However, *N.* (*T.*) *merianii-obtusa* is a
547 fossil species, and its ecology is only inferred from a related extant species. Although
548 *Lychnothamnus barbatus* is living today, it is possible that its ecological preferences have
549 changed since the Miocene. In contrast, several species of the aquatic molluscs suggest a much
550 warmer climate, since they are still living in the Zahle region today, and this region is presently
551 characterized by a hot-summer Mediterranean climate. The ostracod taxa found within the Zahle
552 sequence have broad temperature tolerances, although they are not inconsistent with warmer
553 temperatures, and would thus tend to support the climatic inferences drawn from the aquatic
554 molluscs.

555 All of the groups of aquatic fossils (charophytes, aquatic molluscs and ostracods) include
556 elements that are tolerant of elevated salinity; this is especially true for the ostracods. Elevated
557 salinity in athalassic lakes is often associated with a more arid climate: although the dissolution
558 of evaporitic rocks within a lake catchment can also contribute to elevated salinity, the absence
559 of evaporites from the Zahle region suggests that climate was the more likely control. The land
560 snails from the upper part of the section 3 point to a shift toward a humid environment and thus
561 suggest less dry conditions as today.

562 Data from elsewhere within the Near East, NE Africa and the Arabian Peninsula, point to
563 a regionally-complex pattern of climate in the late Miocene. Kingston and Hill's (1999)
564 reconstructions of the late Miocene vegetation on the Arabic Peninsula included wooded
565 grasslands, consistent with more humid conditions. Palynological analysis from central and
566 western Turkey indicated that this region was dominated by relatively open, grass-dominated

habitats (Akgün et al., 2007), with a climatic cooling and a shift from subtropical to warm temperate conditions at the transition between the middle and late Miocene in central Anatolia, although accompanied by a significant decrease in precipitation (Akkiraz et al., 2011). Griffin (2002) reconstructed more arid conditions in North-eastern Africa during the late Miocene. Globally, the late Miocene witnessed a significant cooling after the mid-Miocene climate optimum, but it was still considerably warmer than today (Herbert et al., 2016). Reconstructions of global vegetation for the Tortonian suggest warm-temperate mixed forests to temperate deciduous forests for the Levantine region (Pound et al., 2011).

7. Conclusion

Non-marine Neogene deposits in the western margin of the Bekaa Valley (Lebanon) near the village of Zahle have been analyzed from the sedimentological and micropalaeontological viewpoints. Three stratigraphic sections were raised with the aim to ascertain the palaeoenvironmental evolution of the area. Facies analysis of the three studied sections indicates that the western margin of the basin was occupied by an alluvial fan that evolved vertically into a perennial lake grading upwards into palustrine conditions. The well-preserved microfossil assemblage recovered from lacustrine and palustrine deposits of Zahle shed new light about the limnological characteristics of this paleolake. During the Miocene the south of the Bekaa Valley was flooded by a perennial, relatively shallow and oligotrophic freshwater lake that evolved to a very shallow and eutrophic lake with a dense palustrine vegetation belt. Ostracod assemblage suggests that oligohaline conditions may prevailed in some periods. However, the absence of evaporite bedrock in the valley's catchment area suggests that climatic change were

589 the main factor controling the salinity of the paleolake. The increase of salinity was probably
590 related to higher evaporation rates during dry periods. Later on, this perennial lake changed into
591 very shallow conditions were eutrophic and palustrine vegetated margins prevailed. In these
592 conditions the lake was subjected to water table fluctuations and episodes of subaerial exposure
593 probably related to changes in the hydrologic budget or climatic changes affecting the Valley
594 during the Miocene. The subsequent high tectonic activity in the area displaced the basin
595 depocenter towards the south leaving the studied deposits exposed along the south western
596 margin of the Valley. The fossil assemblages are somewhat ambiguous indicators of
597 palaeotemperature. Despite some fossil indicators of cold temperatures similar to those of
598 present-day boreal environments, most of the evidence is consistent with temperatures being
599 broadly similar to those of the present-day Zahle region, following a climatic deterioration in the
600 region during the middle-late Miocene. Of course, it is difficult to provide a general overview of
601 the basin and climate evolution based solely on sedimentological/palaeontological analyses of
602 one limited area. Additional data from other localities along the Bekaa Valley are required to
603 expand our knowledge of basin and climate evolution as well as tectonic activity. Unfortunately,
604 the present political situation renders field campaigns in the eastern areas of the basin close to the
605 Syrian border is not advisable for safety reasons.

606 **Acknowledgments**

607 This study was funded by the URB project of the American University of Beirut entitled:
608 "Fossil Charophytes from Lebanon" (Project number AUB-23936). Peter Glöer and Adrienne
609 Jochum are thanked for sharing ideas on the identifications of some of the gastropods. We
610 acknowledge Isaac Casanovas, Raquel López-Antoñanzas and Werner Schwarzhans for their

help in the identification of vertebrate remains and Elsa Gliozzi and Dave Horne for invaluable discussions about the ostracods. We are also very thankful to Rania Shatila (Central Research Science Laboratory of the American University of Beirut) and Jim Davy (Department of Earth Sciences, University College London) for their help and technical support during the SEM sessions. T.A.N. was supported by an Alexander-von-Humboldt Scholarship for Postdoctoral Researchers. Carles Martín-Closas and two anonymous reviewers greatly improved the manuscript.

References

Akgün, F., Kayseri, M.S., Akkiraz, M.S., 2007. Paleoclimatic evolution and vegetational changes during the Late Oligocene–Miocene period in Western and Central Anatolia, Turkey. Palaeogeography, Palaeoclimatology, Palaeoecology 253 (1–2), 56–90.

Akkiraz, M.S., Akgün, F., Utescher, T., Bruch, A.A., Mosbrugger, V., 2011. Precipitation gradients during the Miocene in Western and Central Turkey as quantified from pollen data. Palaeogeography, Palaeoclimatology, Palaeoecology 304, 276–290.

Alqudah, M., Ali Hussein, M., Van den Boorn, S., Podlaha, O.G., Mutterlose, J., 2014. Calcareous nannofossils biostratigraphy of oil shales from Jordan. GeoArabia 19 (1), 117–140.

Alonso-Zarza, A.M., 2003. Palaeonvironmental significance of palustrine carbonates and calcretes in the geological record. Earth Science Reviews 60, 261–298.

Alonso-Zarza, A.M., Wright, V.P., 2010. Palustrine Carbonates. In: Alonso-Zarza, A.M., Tanner, L.H. (Eds.), Carbonates in Continental Settings. Facies, Environments and Processes: Developments in Sedimentology, 61. Elsevier, Amsterdam, pp. 103–126.

633 Alsharhan, A.S., Nairn A.E.M., 1997. Sedimentary basins and petroleum geology of the Middle
634 East. Elsevier, Amsterdam, 843 pp.
635 Anadón, P., Gliozzi, E., Mazzini, I., 2002. Palaeoenvironmental reconstruction of marginal
636 marine environments from combined palaeoecological and geochemical analyses on
637 ostracods. In: Holmes, A., Chivas, A.R. (Eds.), The Ostracoda: Applications in
638 Quaternary Research. Geophysical Union Geophysical Monograph. American
639 Geophysical Union, Washington DC, pp. 227–247.
640 Arconada, B., Ramos, M.A., 2006. Revision of the Genus *Islamia* Radoman, 1973 (Gastropoda,
641 Caenogastropoda, Hydrobiidae) on the Iberian Peninsula and Description of Two New
642 Genera and Three New Species. Malacologia 48 (1/2), 77–132.
643 Bailly, G., Schaefer, O., 2010. Guide illustré des Characées du nord-est de la France. Besançon,
644 France: Conservatoire Botanique National de Franche-Comté. 96 pp.
645 Bank, R.A., Butot, L.J.M., 1984. Some more data on *Hydrobia ventrosa* (MONTAGU, 1803)
646 and "*Hydrobia*" *stagnorum* (GMELIN, 1791) with remarks on the genus *Semisalsa*
647 Radoman, 1974 (Gastropoda, Prosobranchia, Hydrobioidea). Malakologische
648 Abhandlungen. Staatliches Museum für Tierkunde Dresden 10 (2), 5–15.
649 Beydoun, Z.R., 1999. Evolution and development of the Levant (Dead Sea Rift) Transform
650 System: a historicalchronological review of a structural controversy. In: Mac Niocaill, C.,
651 Rayan, P.D. (Eds.), Continental tectonics. Geological Society, London Special
652 Publication 164, 239–255.
653 Bodon, M., Manganelli, G., Giusti, F., 2001. A survey of the European valvatiform hydrobiid
654 genera, with special reference to *Hauffenia* Pollonera, 1898 (Gastropoda: Hydrobiidae).
655 Malacologia 43, 103–215.

656 Boggs, S. Jr., 2011. Principles of Sedimentology and Stratigraphy. Fifth Edition. Pearson,
657 Prentice Hall Inc., 585 pp.
658 Boomer, I., Frenzel, P., Feike, M., 2017. Salinity-driven size variability in *Cyprideis torosa*
659 (Ostracoda, Crustacea). Journal of Micropaleontology 36, 63–69.
660 Boomer, I., Horne, D.J., Slipper, I., 2003. The use of ostracods in paleoenvironmental studies, or
661 what can you do with an ostracod shell? In: Park, L.E., Smith, A.J. (Eds.), Bridging the
662 Gap: Trends in the Ostracode Biological and Geological Sciences. The Paleontological
663 Society Papers, 9. Yale University, New Haven, 153–180.
664 Bößneck, U., 2011. New records of freshwater and land molluscs from Lebanon (Mollusca:
665 Gastropoda & Bivalvia). Zoology in the Middle East 54, 35–52.
666 Ciangherotti, A., Esu, D., Martinetto, E., Giuntelli, P., 2007. The remarkable Middle Pliocene
667 non-marine mollusc record from Ceresole d'Alba, Piedmont, north-west Italy:
668 Biochronology, palaeobiogeography and palaeoecology supported by fossil plants.
669 Geobios 40, 573–587.
670 Corillion, R., 1972. Les Charophycées de France et d'Europe Occidentale. Travaux du
671 laboratoire de botanique de la Faculté des Sciences d'Angers, Angers 11–12, 1–499.
672 De Deckker, P., 2002. Ostracod palaeoecology. In: Holmes, J.A., Chivas, A.R. (Eds.), The
673 Ostracoda: Applications in Quaternary Research. AGU, pp. 121–134.
674 De Deckker, P., Lord, A.R., 2017. *Cyprideis torosa*: a model organism for the Ostracoda?
675 Journal of Micropalaeontology 36 (1), 3–6.
676 Delicado, D., Machordom, A., Ramos, M.A., 2015. Effects of habitat transition on the
677 evolutionary patterns of the microgastropod genus *Pseudamnicola* (Mollusca,
678 Hydrobiidae). Zoologica Scripta 44 (4), 403–417.

679 Dubertret, L., 1945. Carte Géologique au 50000-Feuille de Zahle. Republique Libanaise.
680 Ministère des Travaux Publics.
681 Dubertret, L., 1955. Carte Géologique au 200000-Feuille de Beyrouth. Republique Libanaise,
682 Ministère des Travaux Publics.
683 Dux, F.W., Chivas, A.R., Garcia, A., 2015. Trace-element and stable-isotope chemistry of
684 gyrogonites of the euryhaline charophyte *Lamprothamnium*. Aquatic Botany 120, 51–59.
685 Feist, M., Grambast-Fessard, N., Guerlesquin, M., Karol, K., Lu, H., McCourt, R.M., Wang, Q.,
686 Shenzen, Z., 2005. Treatise on Invertebrate Palaeontology. Part B, Protoctista 1.
687 Charophyta, volume 1. The Geological Society of America, Lawrence, Kansas. 170 pp.
688 Frenzel, P., Ewald, J., Pint, A., 2017. Salinity-dependent sieve pore variability in *Cyprideis*
689 *torosa*: an experiment. Journal of Micropalaeontology 36, 57–62.
690 Frenzel, P., Schulze, I., Pint, A., 2012. Noding of *Cyprideis torosa* valves (Ostracoda) – a proxy
691 for salinity? New data from field observations and a long-term microcosm experiment.
692 International Review of Hydrobiology 97, 314–329.
693 García, A., Chivas, A.R., 2006. Diversity and ecology of extant and Quaternary Australian
694 charophytes (Charales). Cryptogamie Algologie 27(4), 323–340.
695 Gastaldo, R. A., Pfefferkorn, H.W., DiMichele, W. A., 1995. Taphonomic and sedimentologic
696 characterization of roof-shale floras. Geological Society of America 185, 341–352.
697 Germain, L., 1921. Mollusques terrestres et fluviatiles de Syrie. Tome premier - Introduction et
698 Gastéropodes. J.-B. Bailliére et fils, Paris.
699 Gierlowski-Kordesch, E.H., 2010. Lacustrine carbonates. In: Alonso-Zarza, A.M., Tanner, L.H.
700 (Eds.), Carbonates in Continental Settings. Facies, Environments and Processes:
701 Developments in Sedimentology, 61. Elsevier, Amsterdam, pp. 1–101.

Gliozzi, E., Rodriguez-Lazaro, J., Pipik, R., 2017. The Neogene Mediterranean origin of *Cyprideis torosa* (Jones, 1850). Journal of Micropalaeontology 36, 80–93.

Glöer, P., 2002. Die Süßwassergastropoden Nord- und Mitteleuropas. Bestimmungsschlüssel, Lebensweise, Verbreitung. ConchBooks, Hackenheim, 327 pp.

Glöer, P., Bouzid, S., Boeters, H.D., 2010. Revision of the genera *Pseudamnicola* PAULUCCI 1878 and *Mercuria* BOETERS 1971 from Algeria with particular emphasis on museum collections (Gastropoda: Prosobranchia: Hydrobiidae). Archiv für Molluskenkunde 139 (1), 1–22.

Gomez, F., Khawlie, M., Tabet, C., Darkal, A. N., Khair, K., Barazangi, M. 2006. Late Cenozoic uplift along the northern Dead Sea transform in Lebanon and Syria. Earth and Planetary Science Letters 241, 913–931.

Goodfriend, G.A., 1992. The use of land snail shells in paleoenvironmental reconstruction. Quaternary Science Reviews 11, 665–685. DOI: 10.1016/0277-3791(92)90076-K

Gradstein, F.M., Ogg, J.G., Schmitz, M.D., Ogg, G.M. (Eds.) 2012. The Geologic Time Scale 2012, 2 volumes. Elsevier, Oxford.

Griffin, D.L., 2002. Aridity and humidity: Two aspects of the late Miocene climate of North Africa and the Mediterranean. Palaeogeography, Palaeoclimatology, Palaeoecology 182, 65–91.

Grossi, F., Gliozzi, E., Anadón, P., Castorina, F., Voltaggio, M., 2015. Is *Cyprideis agrigentina* Decima a good paleosalinometer for the Messinian Salinity Crisis? Morphometrical and geochemical analyses from the Eraclea Minoa section (Sicily). Palaeogeography Palaeoclimatology, Palaeoecology 419, 75–89.

724 Harzhauser, M., Neubauer, T.A., 2018. Opole (Poland) – a historical key locality for middle
725 Miocene terrestrial mollusc faunas. Bulletin of Geosciences 93, 71–146. DOI:
726 10.3140/bull.geosci.1692
727 Heller, J., 2009. Land snails of the land of Israel. Natural History and a field guide. Pensoft
728 Publishers, Sofia. 360 pp.
729 Heip, C., 1976. The life-cycle of *Cyprideis torosa* (Crustacea, Ostracoda). Oecologia 24, 229–
730 245.
731 Herbert, T.D., Lawrence, K.T., Tzanova, A., Peterson, L.C., Caballero-Gill, R., Kelly, C.S.,
732 2016. Late Miocene global cooling and the rise of modern ecosystems. Nature
733 Geoscience 9, 843–847. DOI: 10.1038/ngeo2813
734 Horne, D.J., Curry, B.B. & Mesquita-Joanes, F. 2012. Mutual climatic range methods for
735 Quaternary ostracods. In: Horne, D.J., Holmes, J.A., Rodriguez-Lazaro, J. & Viehberg ,
736 F.A. (Eds.) Ostracoda as Proxies for Quaternary Climate Change. Developments in
737 Quaternary Science 17, 65-84. Elsevier.
738 Kansou, M., 1961. Découverte de vertébrés pontiens au Liban dans la plaine de la Békaa. Bull.
739 Sci. Cons. Acad. RPF Yougoslavie 6, 65 pp.
740 Keyser, D., 2005. Histological peculiarities of the noding process in *Cyprideis torosa* (Jones)
741 (Crustacea, Ostracoda). Hydrobiologia 538, 95–106.
742 Kingston, J., Hill, A., 1999. Late Miocene Palaeoenvironments in Arabia: a synthesis. In:
743 Whybrow, P.J., Hill, A. (Eds.), Fossil Vertebrates of Arabia: with Emphasis on the Late
744 Miocene Faunas, Geology, and Palaeoenvironments of the Emirate of Abu Dhabi, United
745 Arab Emirates. Yale University Press, New Haven, 389–407.

746 Krause, W., 1985. Uber die Standortsanspruche und das Ausbreitungsverhalten der Stern-
747 Armleuchteralge *Nitellopsis obtusa* (Desvaux) J. Groves. Carolinea 42, 31–42.
748 Krause, W., 1997. Charales (Charophyceae). Süsswasserflora von Mitteleuropa. Band 18. Gustav
749 Fischer Verlag, Jena: 1–202.
750 Larkin, D.L., Monfils, A.K., Boissezon, A., Sleith, R.S., Skawinski, P.M., Welling, C.H., Cahill,
751 B.C., Karol, K.G., 2018. Biology, ecology, and management of starry stonewort
752 (*Nitellopsis obtusa*; Characeae): A Red-listed Eurasian green alga invasive in North
753 America. Aquatic Botany 148, 15–24.
754 Lateef, A.S., 2003. Quaternary terrestrial stratigraphic correlations between the Levant and the
755 circum-North Atlantic region: current knowledge and constraints. Studia Quaternaria 20,
756 61–72.
757 Lateef, A.S., 2007. Geological history of the Bekaa Valley. Second International Conference on
758 the Geology of the Tethys, Cairo University, pp. 391–402.
759 Ligios, S., Gliozzi, E., 2012. The genus *Cyprideis* Jones, 1857 (Crustacea, Ostracoda) in the
760 Neogene of Italy: a geometric morphometric approach. Revue de Micropaléontologie 55,
761 171–207.
762 López-Antoñanzas, R., Knoll, F., Maksoud, S., Azar, D., 2015. First Miocene rodent from
763 Lebanon provides the 'missing link' between Asian and African gundis (Rodentia:
764 Ctenodactylidae). Scientific Reports 5, 12871. DOI: 10.1038/srep12871
765 Ložek, V., 1964. Quartärmollusken der Tschechoslowakei. Rozpravy Ústredního ústavu
766 geologického 31, 1–374.
767 Malez, M., Forsten, A., 1989. *Hipparion* from the Bekaa valley of Lebanon. Geobios 22, 665–
768 670.

769 Martín-Closas, C., Wojcicky, J.J., Fonollà, L., 2006. Fossil charophytes and hydrophytic
770 angiosperms as indicators of lacustrine trophic change. A case study in the Miocene of
771 Catalonia (Spain). Cryptogamie-Algologie 27, 357–379.
772 Meisch, C., 2000. Freshwater Ostracoda of Western and Central Europe. Süßwasserfauna von
773 Mitteleuropa 8/3. Spektrum Akademischer Verlag, Heidelberg.
774 Mesquita-Joanes, F., Smith, A.J., Viehberg, F., 2012. The ecology of Ostracoda across levels of
775 biological organisation from individual to ecosystem: a review of recent developments
776 and future potential. In: Horne, D.J., Holmes, J.A., Rodriguez-Lazaro, J., Viehberg, F.
777 (Eds.), Ostracoda as Proxies for Quaternary Climate Change, Developments in
778 Quaternary Science 17. Elsevier, pp. 15–35.
779 Müller, C., Higazi, F., Hamdan, W., Mroueh, M., 2010. Revised stratigraphy of the Upper
780 Cretaceous and Cenozoic series of Lebanon based on nannofossils. Geological Society,
781 London, Special Publications 341, 287–303.
782 Neubauer, T.A., Harzhauser, M., Mandic, O., Jovanović, G., 2017. The late middle Miocene
783 non-marine mollusk fauna of Vračević (Serbia): filling a gap in Miocene land snail
784 biogeography. Bulletin of Geosciences 91, 731–778. DOI: 10.3140/bull.geosci.1639
785 Pilsbry, H.A., 1927–1935. Manual of Conchology, Second Series: Pulmonata, 28. Geographic
786 Distribution of Pupillidae; Strobilopsidae, Valloniidae and Pleurodiscidae. Academy of
787 Natural Sciences of Philadelphia, Philadelphia.
788 Pint, A., Frenzel, P., 2016. Ostracod fauna associated with Cyprideis torosa - an overview.
789 Journal of Micropalaeontology 36, 113–119. DOI: 10.1144/jmpaleo2016-010

790 Pint, A., Frenzel, P., Fuhrmann, R., Scharf, B., Wennrich, V., 2012. Distribution of *Cyprideis*
791 *torosa* (Ostracoda) in Quaternary athalassic sediments in Germany and its application for
792 palaeoecological reconstructions. International Review of Hydrobiology 97, 330–355.
793 Pelechaty, M., Brozowski, M., Karol, P., 2017. Overwintering and gyrogonite formation by the
794 rare and endangered indicative macroalga *Lychnothamnus barbatus* (Meyen) Leonh. in
795 eutrophic conditions. Aquatic Botany 139, 19–24.
796 Ponikarov, V.P., 1967. The geology of Syria: explanatory notes on the geologic map of Syria,
797 scale 1: 500 000. Part I Stratigraphy, igneous rocks and tectonics. Ministry of Industry,
798 Damascus.
799 Pound, M.J., Haywood, A.M., Salzmann, U., Riding, J.B., Lunt, D.J., Hunter, S.J., 2011. A
800 Tortonian (Late Miocene, 11.61–7.25 Ma) global vegetation reconstruction.
801 Palaeogeography, Palaeoclimatology, Palaeoecology 300, 29–45.
802 Radea, C., Parmakelis, A., Vardinoyannis, S., Vardinoyannis, K., 2017. A new *Islamia* species
803 (Gastropoda: Hydrobiidae) from Cyprus. Folia Malacologica 25, 231–236. Rodriguez-
804 Lazaro, J., Ruiz-Muõz, F., 2012. A General Introduction to Ostracods: Morphology,
805 Distribution, Fossil Record and Applications In: Horne, D.J., Holmes, J.A., Rodriguez-
806 Lazaro, J., Viehberg, F. (Eds.), Ostracoda as Proxies for Quaternary Climate Change,
807 Developments in Quaternary Science 17. Elsevier, pp. 1–14.
808 Ruiz, F., Abad, M., Bodergat, A.M., Carbonel, P., Rodríguez-Lázaro, J., González Regalado,
809 M.L., Toscano, A., García, E.X., Prenda, J., 2013. Freshwater ostracods as
810 environmental tracers. International Journal of Environmental Science and Technology
811 10, 1115–1128.

812 Salvador, R.B., Pippèrr, M., Reichenbacher, B., Rasser, M.W., 2016. Early Miocene continental
813 gastropods from new localities of the Molasse Basin in southern Germany.
814 Paläontologische Zeitschrift 90, 469–491. Sanjuan, J., Alqudah, M., 2018. Charophyte
815 flora from Miocene deposits of Zahle (Beeka Valley, Lebanon). Biostratigraphic,
816 palaeoenvironemental and palaeobiogeographical implications. Geodiversitas 40 (10),
817 195–209.
818 Sanjuan, J., Martín-Closas, C., 2012. Charophyte palaeoecology in the Upper Eocene of the
819 Eastern Ebro Basin (Catalonia, Spain). Biostratigraphic implications. Palaeogeography,
820 Palaeoclimatology, Palaeoecology 365–366, 247–262.
821 Sanjuan, J., Martín-Closas, C., 2015. Biogeographic history of two Eurasiatic Cenozoic
822 charophyte lineages. Aquatic Botany 120 (A), 18–31.
823 Sanjuan, J., Martín-Closas, C., Costa, E., Barberà, X., Garcés, M., 2014. Calibration of Eocene-
824 Oligocene charophyte biozones in the Eastern Ebro Basin (Catalonia, Spain).
825 Stratigraphy 11 (1), 61–81.
826 Sanjuan, J., Vicente, A., Flor-Arnau, N., Cambra, J., 2017. Effects of light and temperature on
827 *Chara vulgaris* gyrogonite productivity and polymorphism. Palaeoenvironmental
828 implications. Phycologia 56 (2), 204–212.
829 Seddon, M.B., 2014. *Gyraulus hebraicus*. The IUCN Red List of Threatened Species 2014:
830 e.T164820A1075506. http://dx.doi.org/10.2305/IUCN.UK.2014-
831 1.RLTS.T164820A1075506.en. Accessed on 24 November 2017.
832 Şereflişan, H., Yıldırım, M.Z., Şereflişan, M., 2009. The gastropod fauna and their abundance,
833 and some physicochemical parameters of Lake Gölbaşı (Hatay, Turkey). Turkish Journal
834 of Zoology 33, 287–296.

835 Soulié-Märsche, I., 1989. Étude comparée de gyrogonites de charophytes actuelles et fossiles et
836 phylogénie des genres actuels. Millau, Imprimerie des Tilleuls. 237 pp.
837 Soulié-Märsche, I., Benammi, M., Gemayel, P., 2002. Biogeography of living and fossil
838 *Nitellopsis* (Charophyta) in relationship to new finds from Morocco. Journal of
839 Biogeography 29, 1703–1711.
840 Soulié-Märsche, I., Bieda, S., Lafond, R., Maley, J., Baitoudji, M., Vincent, P.M., Faure, H.,
841 2010. Charophytes as bio-indicators for lake level high stand at "Trou au Natron",
842 Tibesti, Chad, during the Late Pleistocene. Global and Planetary Change 72(4), 334–340.
843 Soulié-Märsche, I., Martín-Closas, C., 2003. *Lychnothamnus barbatus* (charophytes) from the
844 upper Miocene of la Cerdanya (Catalonia, Spain): Taxonomic and palaeoecological
845 implications. Acta Micropalaeontologica Sinica 20 (2), 156–165.
846 Stworzewicz, E., 2009. Miocene land snails from Bełchatów (central Poland). IV: Pupilloidea
847 (Gastropoda Pulmonata). Systematic, biostratigraphic and palaeoecological studies. Folia
848 Malacologica 7(3), 133–170.
849 Szarowska, M., 2006. Molecular phylogeny, systematics and morphological character evolution
850 in the Balkan Rissooidea (Caenogastropoda). Folia Malacologica 14 (3), 99–168.
851 Van Damme, D., 2014. *Melanopsis buccinoidea*. The IUCN Red List of Threatened Species
852 2014: e.T156110A42422389. http://dx.doi.org/10.2305/IUCN.UK.2014–
853 1.RLTS.T156110A42422389.en. Accessed on 18 May 2018.
854 Van Damme, M.B., Kebapçı, U., 2014. *Valvata saulcyi.* The IUCN Red List of Threatened
855 Species 2014: e.T155862A42422803. http://dx.doi.org/10.2305/IUCN.UK.2014–
856 1.RLTS.T155862A42422803.en. Accessed on 18 May 2018.

van Harten, D., 2000. Variable noding in *Cyprideis torosa* (Ostracoda, Crustacea): an overview, experimental results and a model from Catastrophe Theory. Hydrobiologia 419, 131–139.

Vicente, A., Expósito, M., Sanjuan, J., Martín-Closas, C., 2016. Small sized charophyte gyrogonites in the Maastrichtian of Coll de Nargó, Eastern Pyrenees: An adaptation to temporary floodplain ponds. Cretaceous Research 57, 443–456.

Villalba-Breva, S., Martín-Closas, C., 2011. A Characean thallus with attached gyrogonites and associated fossil charophytes from the Maastrichtian of the eastern Pyrenees (Catalonia, Spain). Journal of Phycology 47, 131–143.

Walley, C.D., 1996. The geology and hydrogeology of the Aammiq wetland region. A Rocha Lebanon. 27 pp.

Welter-Schultes, F.W., 2012. European non-marine molluscs, a guide for species identification. Planet Poster Editions, Göttingen. 757 pp.

Whatley, R., 1983. The application of Ostracoda to palaeoenvironmental analysis. In: Maddocks, R.F. (Ed.), Applications of Ostracoda. University of Houston, Houston, pp. 51–77.

Wouters, K., 2017. On the modern distribution of the euryhaline species *Cyprideis torosa* (Jones, 1850) (Crustacea, Ostracoda). Journal of Micropaleontology 36, 21–30.

Yıldırım, M.Z., 1999. Türkiye Prosobranchia (Gastropoda: Mollusca) türleri ve zoocoğrafik yayılışları. 1. Tatlı ve acı sular. Turkish Journal of Zoology 23, 877–900.

878 **Figure Captions**

879 **Figure 1**. Geological sketch of the western part of the Bekaa Valley, Lebanon showing the
880 location of studied section (modified from Sanjuan and Alqudah, 2018).

881 **Figure 2**. Geological map showing the detailed location of the three stratigraphic sections near
882 the town of Zahle. A. section 1, B. Section 2, C. Section 3 (modified from Dubertret, 1945).

883 **Figure 3**. A–B. Microfacies of wackestone–packstone with abundant dissolved gastropod shells
884 (D.S) from a limestone interval at the top of the Zahle section 1 (sample ZL). C–H. Field photos
885 of the stratigraphic sections. C–E. Section 1. C. Base of the lacustrine sequence in Zahle, see the
886 location of sample Z-0 between conglomerate channels (CGL). D. Marls of the lacustrine
887 sequence, see the location of sample Z-1. E. Detail of the dominant facies at the base of the
888 section, high concentration of microgastropods (G.S). F–H. Section 3. F. Dark grey marls at the
889 top of section 3, see the location of sample Z-1. G. Detail of section 3 showing edaphic
890 structures (root marks, R.M) underlying a lignite horizon (L.H). H. Detail of section 3 showing
891 an interval of accumulations of broken large gastropod shells or shell-debris (G.S) of
892 *Melanopsis buccinoidea*.

893 **Figure 4**. Stratigraphic logs for sections 1, 2 and 3 of the lacustrine deposits of Zahle showing
894 their correlation and their facies associations. Z-0 to Z-11 represent the stratigraphic position of
895 samples extracted for microfossils. ZL refers to the stratigraphic position of the sample
896 recovered for microfacies analysis.

897 **Figure 5**. Charophytes from lacustrine deposits of Zahle. **A–C**: *Nitellopsis* (*Tectochara*)
898 *merianii*; sample Z-2 (A. apical view n°2017019 AUBGM, B. lateral view n°2017003 AUBGM,

C. basal view nº2017026 AUBGM). **D–F:** *Lychnothamnus barbatus* var. *antiquus*; sample Z-2 (D. apical view nº2017011 AUBGM, E. lateral view nº2017014 AUBGM, F. basal view nº2017012 AUBGM). **G–J:** *Chara microcera*; sample Z-1 (G. apical view nº2017002 AUBGM, H. lateral view nº2017002 AUBGM, I. lateral view nº2017003 AUBGM, J. basal view nº2017005 AUBGM). **K–N:** *Chara* cf. *globularis*; sample Z-1 (K. apical view nº2017007 AUBGM, L. lateral view nº2017008 AUBGM); sample Z-8 (M. lateral view nº2019001 AUBGM, N. basal view nº2019002 AUBGM). **O–Q:** *Sphaerochara* sp.; sample Z-10 (O. apical view nº2019003 AUBGM, P. lateral view nº2019004 AUBGM, Q. basal view nº2019005 AUBGM).

Figure 6: Molluscs recovered from Miocene lacustrine deposits of Zahle. **A–C**: *Valvata saulcyi*; all from sample Z-8 (A. nº2019006 AUBGM, B. nº2019007 AUBGM, C. nº2019008 AUBGM). **D, E**: *Bithynia* sp. (opercula); both from sample Z-8 (D. nº2019009 AUBGM, E. nº2019010 AUBGM). **F**: *Melanopsis buccinoidea*; sample Z-6 nº2019011 AUBGM. **G, H**: *Semisalsa* sp.; both from sample Z-5 (G. nº2019012 AUBGM, H. nº2019013 AUBGM). **I**: *Pseudamnicola* sp.; sample Z-4 nº2019014 AUBGM. **J**: *Islamia* sp.; sample Z-5 nº2019015 AUBGM. **K**: *Islamia* sp.; sample Z-1 nº2019016 AUBGM. **L**: *Radix* sp.; sample Z-10 nº2019017 AUBGM. **M**: *Gyraulus* cf. *hebraicus*; sample Z-8 nº2019018 AUBGM. **N**: *Gyraulus* cf. *piscinarum*; sample Z-5 nº2019019 AUBGM. **O:** *Gyraulus* cf. *piscinarum*; sample Z-1 nº2019020 AUBGM. **P**: *Carychium* sp.; sample Z-8 nº2019021 AUBGM. **Q:** *Vertigo* cf. *antivertigo*; sample Z-8 nº2019022 AUBGM. **R:** *Strobilops* sp.; sample Z-11 nº2019023 AUBGM . **S–U:** *Pisidium* cf. *moitessierianum* (left valves), all from sample Z-6 (S. nº2019024 AUBGM, T. nº2019025 AUBGM, U. nº2019026 AUBGM) .

Figure 7. Ostracods from lacustrine deposits of Zahle. **A:** *Cyprideis* sp., female, external lateral view of right valve; sample Z-7 nº2019027 AUBGM. **B:** *Cyprideis* sp., female, internal lateral view of right valve; sample Z-7 nº2019028 AUBGM. **C:** *Cyprideis* sp., female, external lateral view of left valve; sample Z-7 nº2019029 AUBGM. **D:** *Cyprideis* sp., female, internal lateral view of left valve; sample Z-7 nº2019030 AUBGM. **E:** *Cyprideis* sp., male, external lateral view of left valve; sample Z-7 nº2019031 AUBGM. **F:** *Cyprideis* sp., male, internal lateral view of left valve; sample Z-7 nº2019032 AUBGM. **G:** *Cyprideis* sp., male, external lateral view of right valve; sample Z-7 nº2019033 AUBGM. **H:** *Cyprideis* sp., male, internal lateral view of right valve; sample Z-7 nº2019034 AUBGM. **I:** *Cyprideis* sp., female, dorsal view of carapace; sample Z-7 nº2019035 AUBGM. **J:** *Cyprideis* sp., male, dorsal view of carapace; sample Z-7 nº2019036 AUBGM. **K:** *Cyprideis* sp., female, external lateral view of right valve, noded form; sample Z-0 nº2019037 AUBGM. **L:** *Cyprideis* sp., female, external lateral view of left valve, noded form; sample Z-5 nº2019038 AUBGM. **M:** *Cyprideis* sp., male, external lateral view of left valve, noded form; sample Z-8 nº2019039 AUBGM. **N:** *Cyprideis* sp., male, external lateral view of right valve, noded form; sample Z-5 nº2019040 AUBGM. **O:** *Cypris pubera*, external lateral view of left valve; sample Z-6 nº2019041 AUBGM. **P:** *Strandesia* sp., external lateral view of right valve; sample Z-1 nº2019042 AUBGM. **Q:** *Candona* cf. *angulata*, male, left valve; sample Z-5 nº2019043 AUBGM.

Figure 8. Palaeoenvironmental model summarizing the distribution of microfossils in the Zahle palaeolake. The main stratigraphic logs (section 1, 2 and 3) are represented in numbers. Not to scale.

Table 1. List of microfossils and their relative abundance recovered from lacustrine deposits of Zahle in the western margin of the Bekaa Valley. This table is based on a semi-quantitative visual estimation of the fossils. Vertical position of samples represents their relative stratigraphic position, which is indicated in the figure 4.

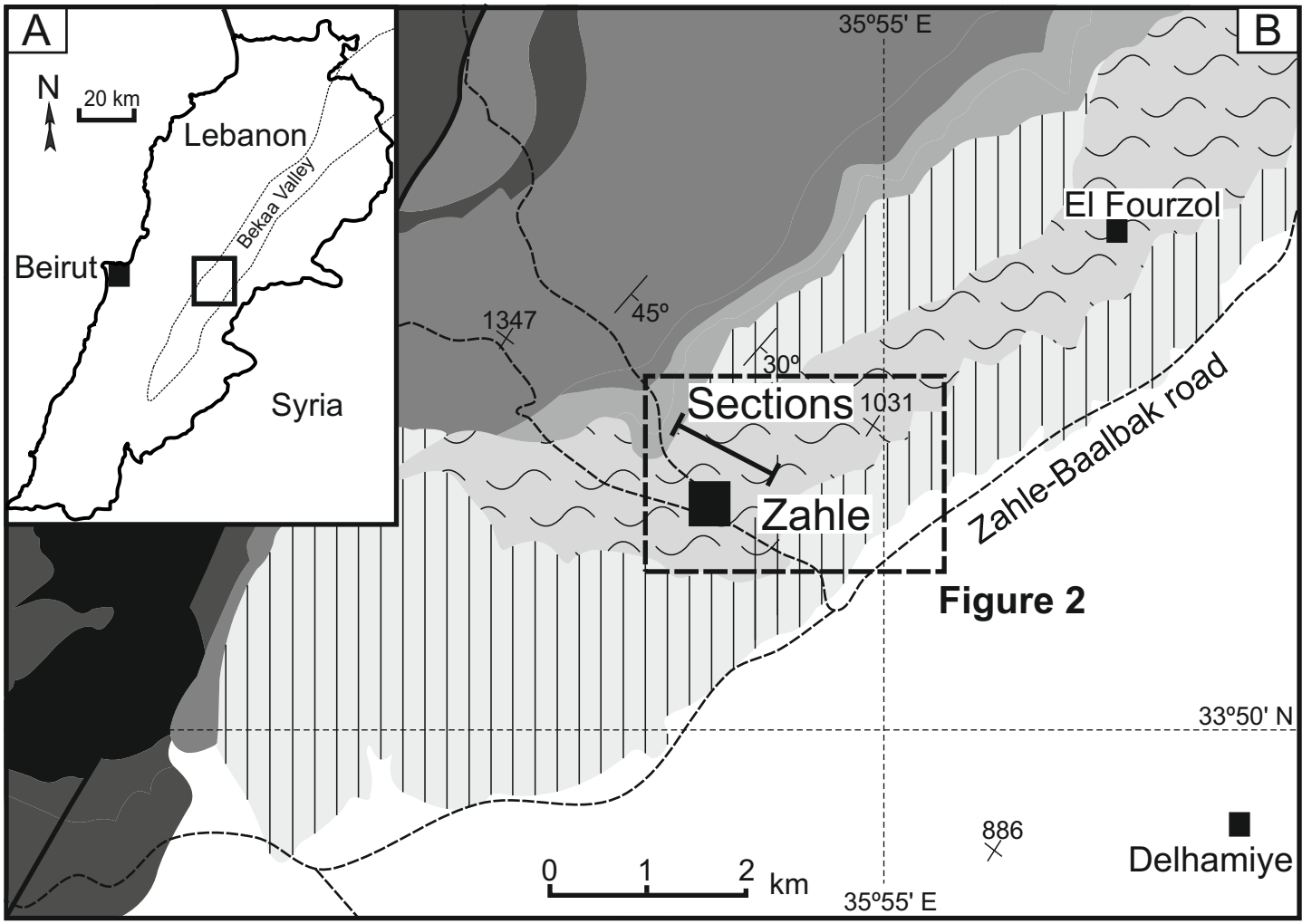

Legend

- Pliocene - Recent (Alluvial)
- Zahle Formation (Lacustrine marl)
- Miocene (Conglomerate)
- Eocene (Nummulitic limestone)
- Upper Cretaceous (Limestone)
- Lower Cretaceous (Marl)
- Jurassic (Limestone)
- Village
- Section
- Road
- Faults
- Dipping
- Elevation point (m)

Figure 1

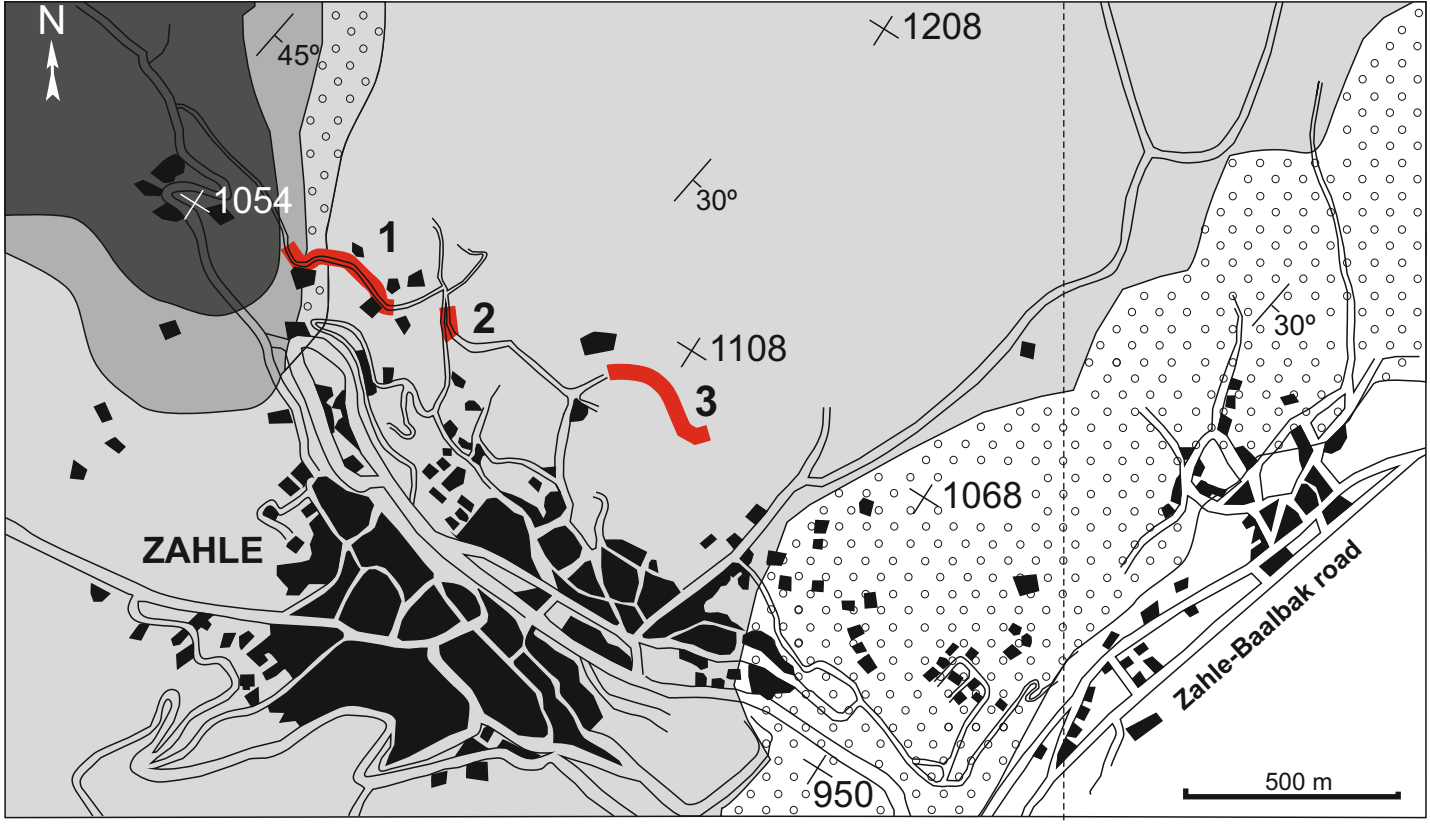

Legend

- Pliocene - Recent (Alluvial)
- Lacustrine marls, limestone and lignites (Miocene)
- Conglomerate and red mudstone (Pliocene)
- Nummulitic limestone (Eocene)
- Limestone (Cretaceous)
- Buildings
- Sections
- Road/streets
- Faults
- Dipping
- Elevation point (m)

Figure 2

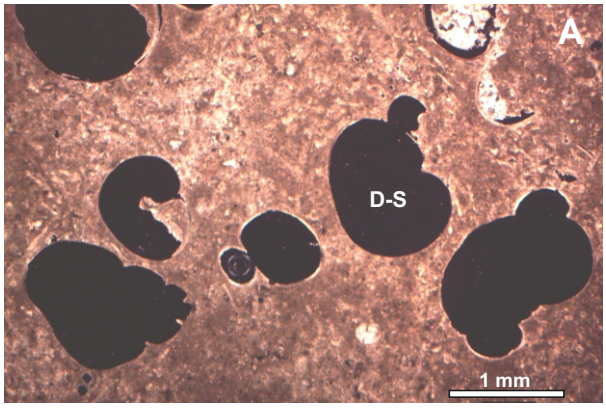
A
D-S
1 mm

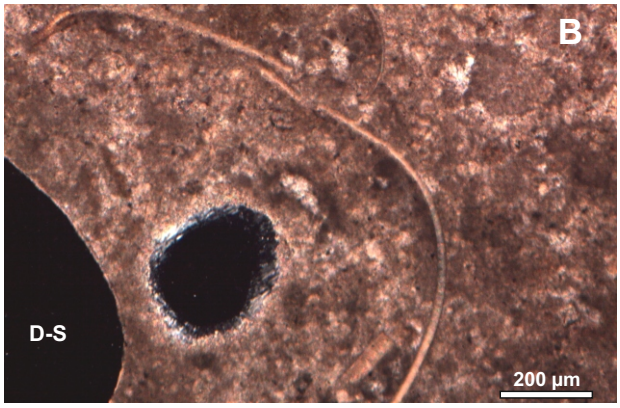
B
D-S
200 µm

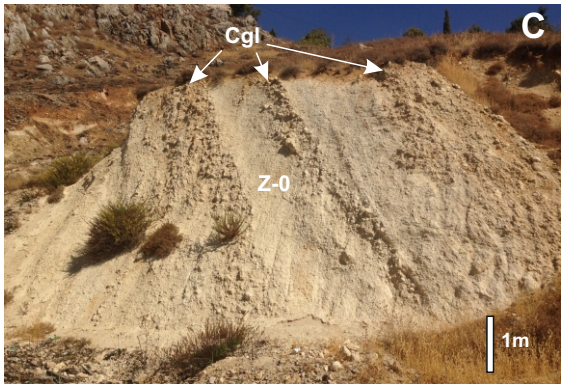
C
Cgl
Z-0
1m


D
Z-1
1m

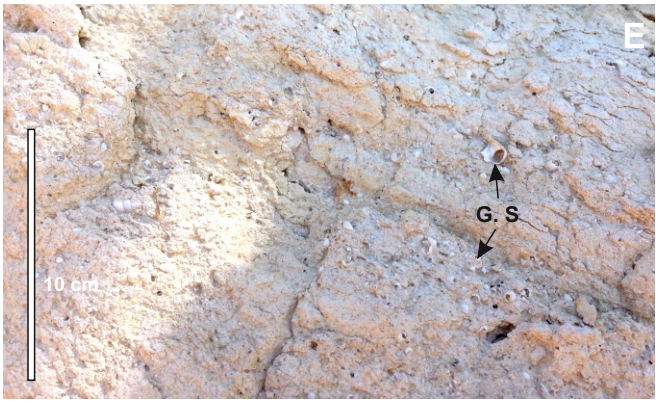
E
G. S
10 cm

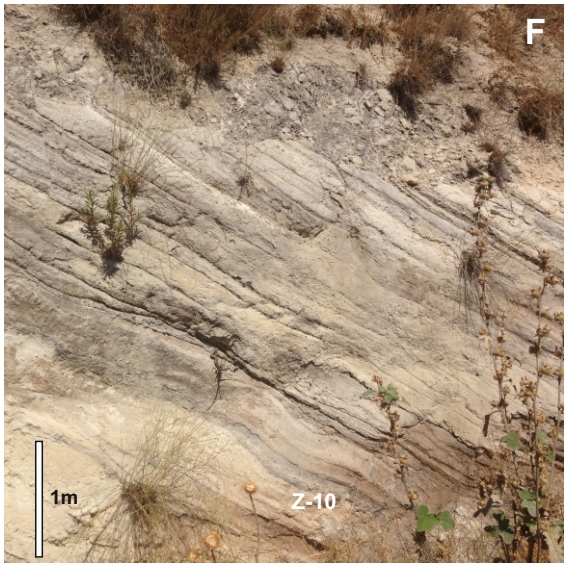
F
1m
Z-10

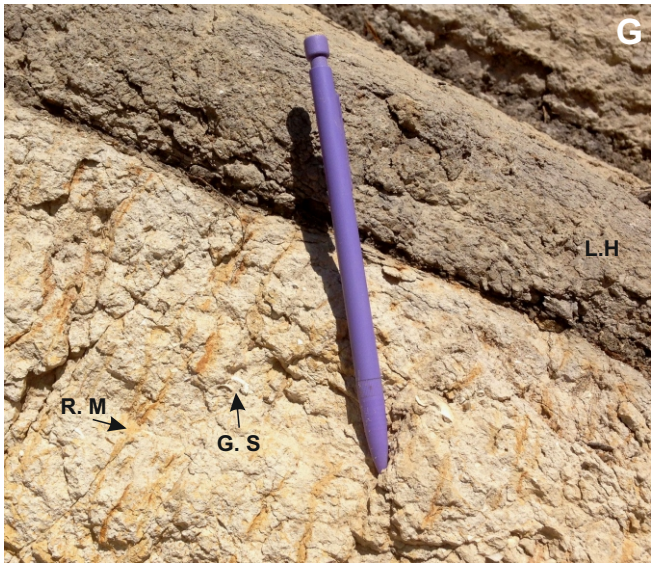
G
L.H
R. M
G. S


H
G. S
NOVOTEL

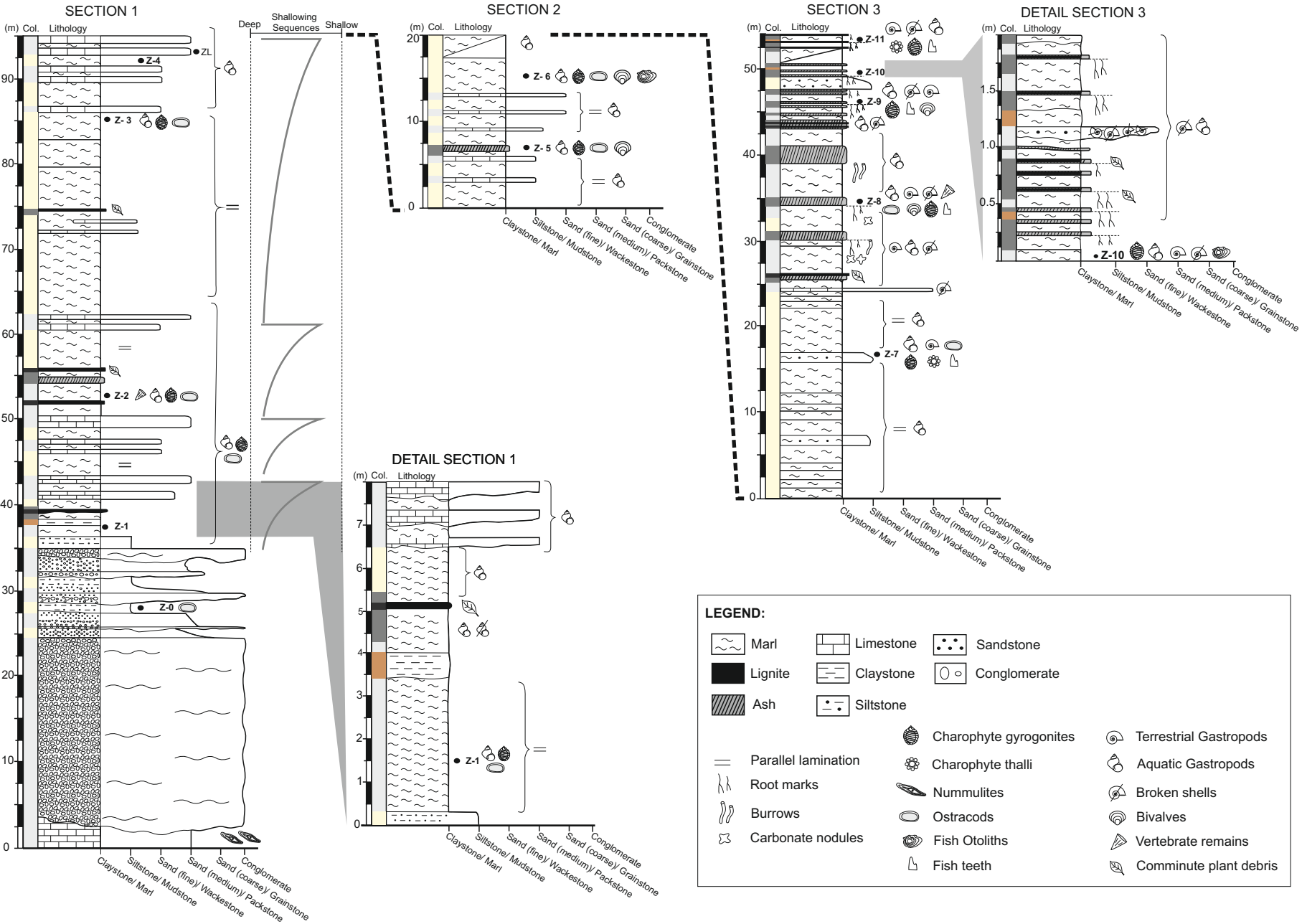
SECTION 1
SECTION 2
SECTION 3
DETAIL SECTION 3
DETAIL SECTION 1
Deep
Shallowing Sequences
Shallow
(m) Col. Lithology
Z-4
ZL
Z- 3
Z-2
Z-1
Z-0
Z- 6
Z- 5
Z-11
Z-10
Z-9
Z-8
Z-7
Claystone/ Marl
Siltstone/ Mudstone
Sand (fine)/ Wackestone
Sand (medium)/ Packstone
Sand (coarse)/ Grainstone
Conglomerate
LEGEND:
Marl
Limestone
Sandstone
Lignite
Claystone
Conglomerate
Ash
Siltstone
Parallel lamination
Root marks
Burrows
Carbonate nodules
Charophyte gyrogonites
Charophyte thalli
Nummulites
Ostracods
Fish Otoliths
Fish teeth
Terrestrial Gastropods
Aquatic Gastropods
Broken shells
Bivalves
Vertebrate remains
Comminute plant debris

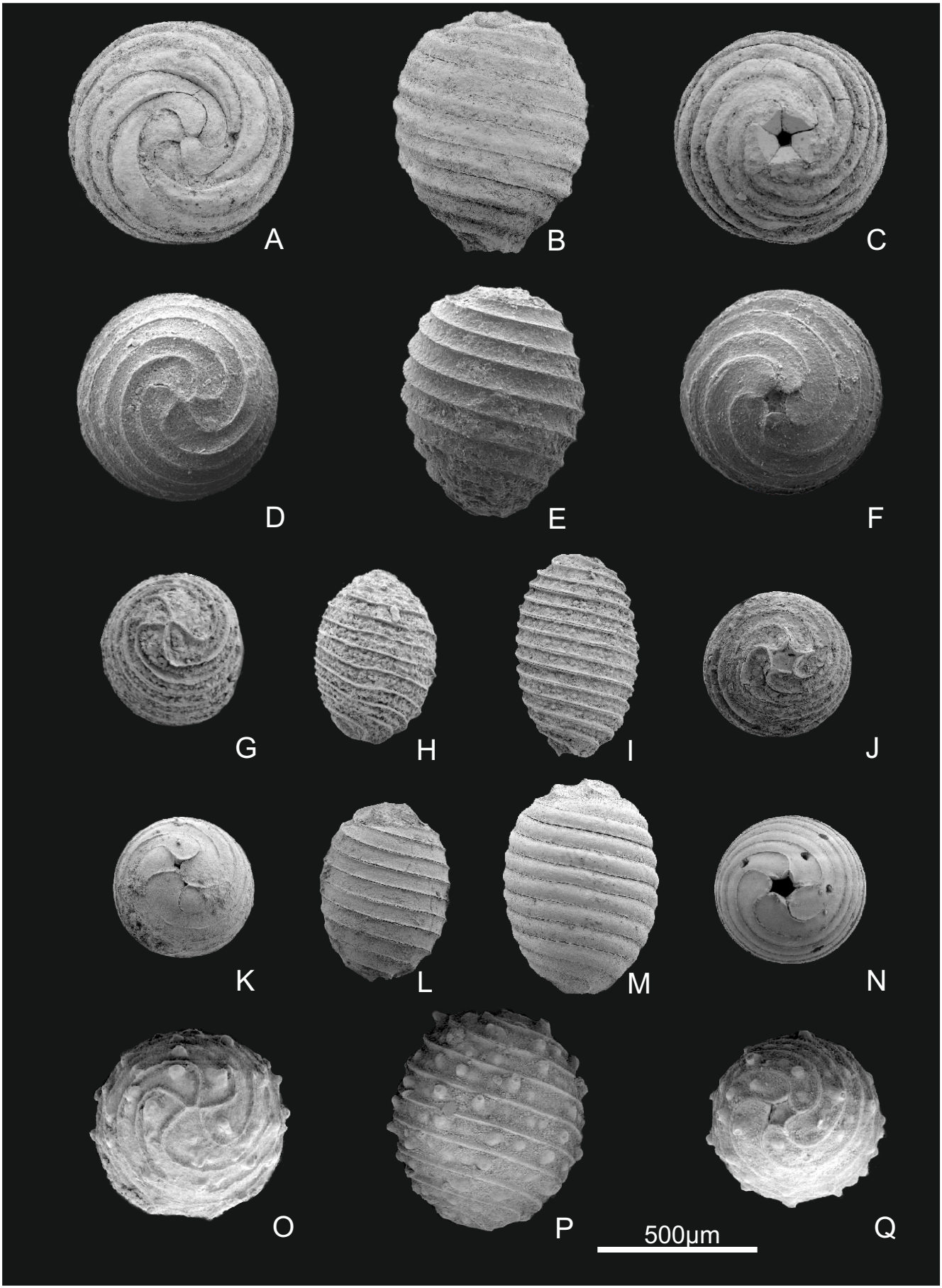
A
B
C
D
E
F
G
H
I
J
K
L
M
N
O
P
Q
500µm

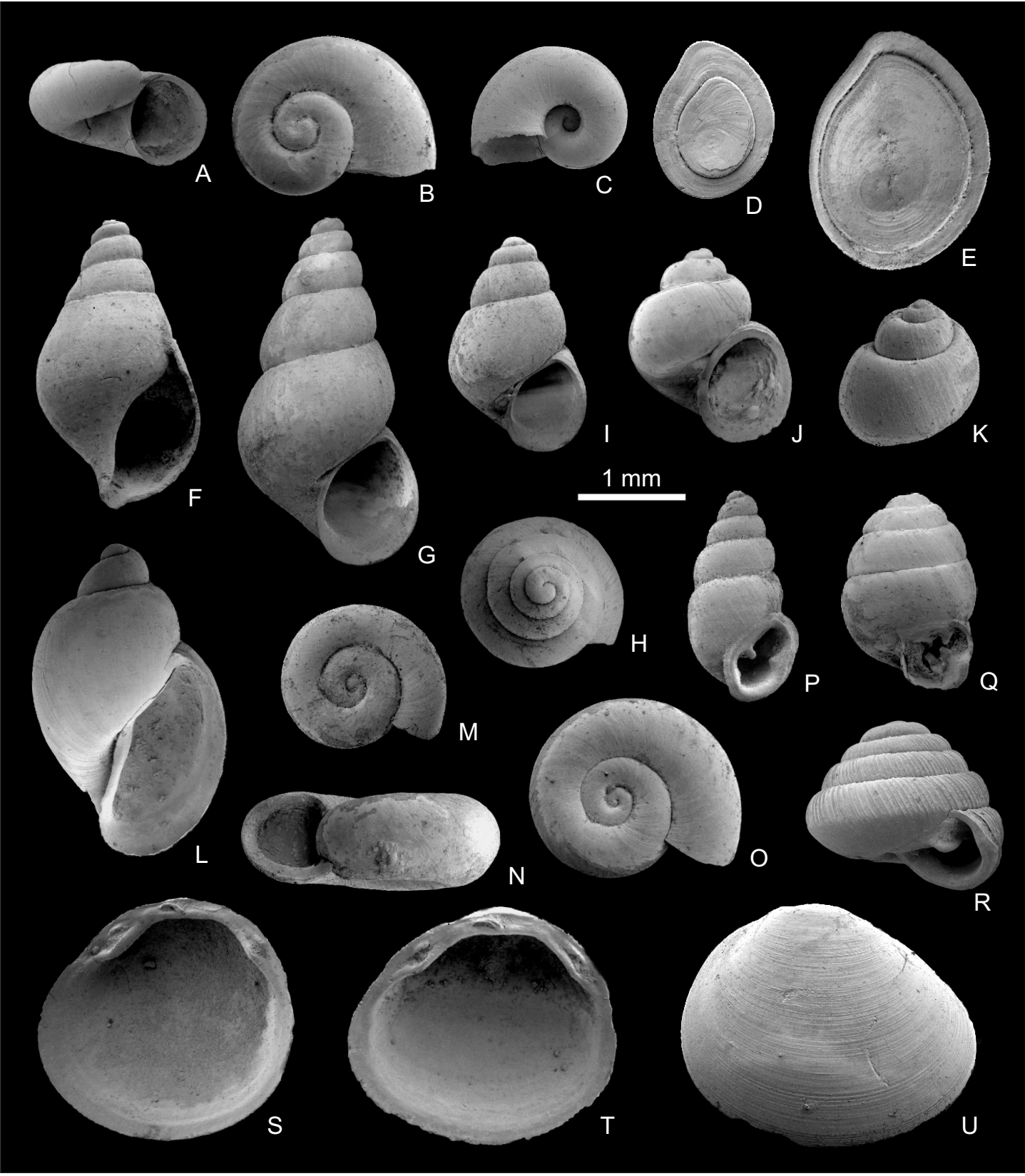
A
B
C
D
E
F
G
I
J
K
1 mm
H
P
Q
L
M
N
O
R
S
T
U

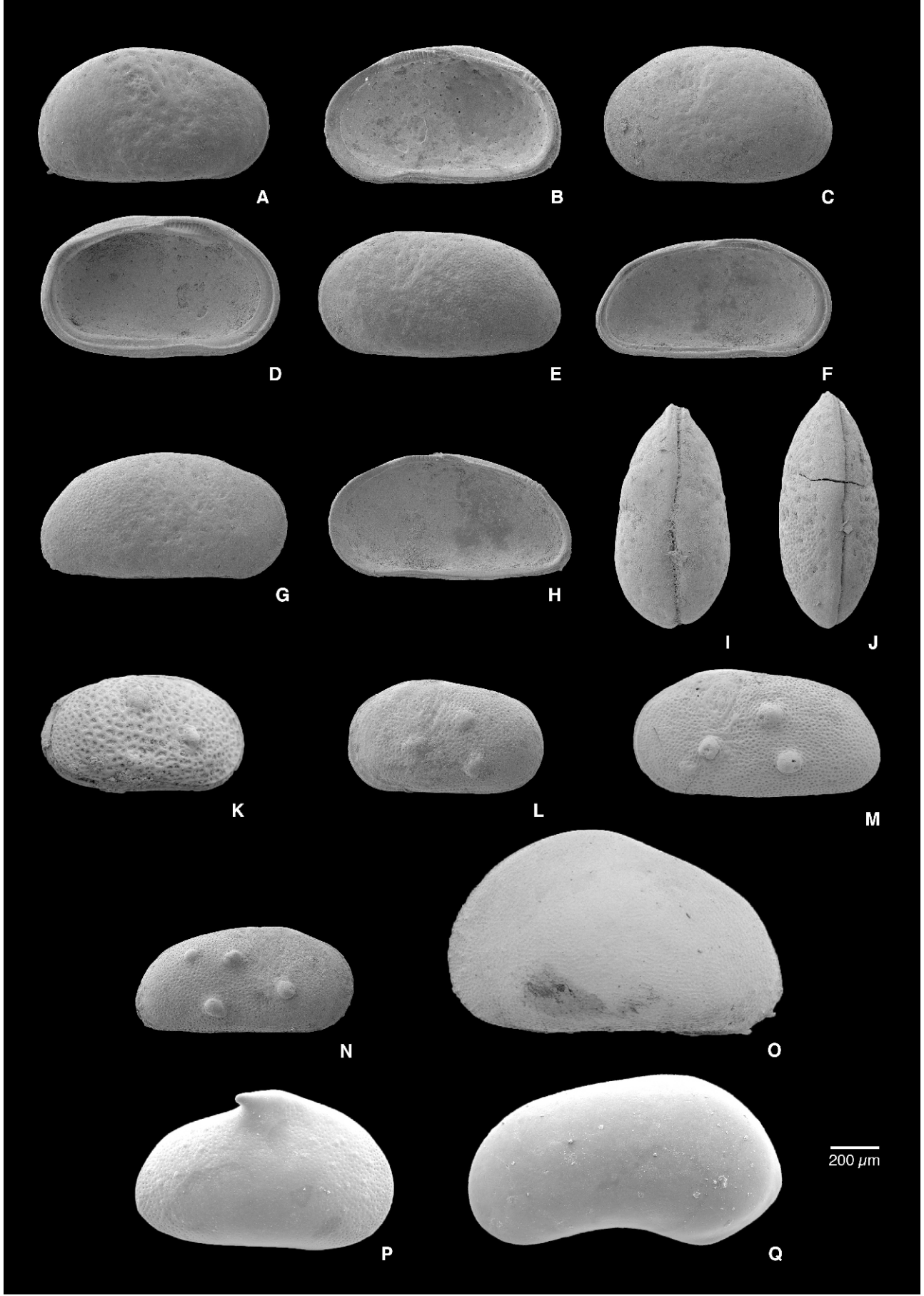
A
B
C
D
E
F
G
H
I
J
K
L
M
N
O
P
Q
200 μm

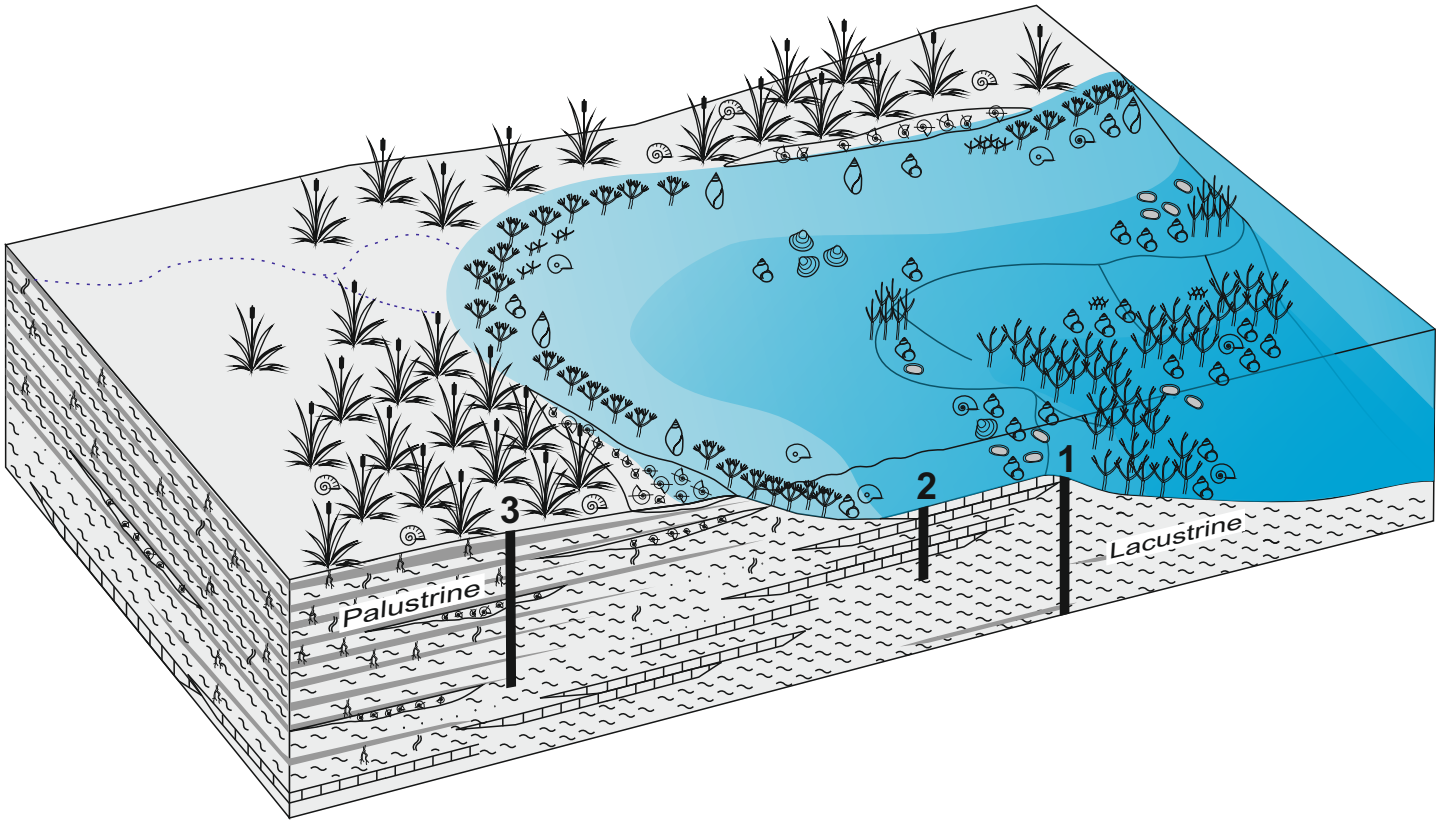

LEGEND:

- Marl
- Limestone
- Organic marls and lignite
- Sandstone
- Shell debris
- Root marks
- Burrows

Gastropods:

- Aquatic (Hydrobiidae)
- Aquatic (Pulmonates)
- Aquatic (*Valvata*)
- Aquatic (*Melanopsis*)
- Terrestrial
- Fragmented shells

- Palustrine helophytic plants

Charophytes:

- *Chara* cf. *globularis*
- *Nitellopsis* (*T.*) *merianii*
- *Lychnothamnus barbatus*
- *Chara microcera*
- *Sphaerochara* sp.

- Bivalve (*Pisidium*)
- Ostracods (*Cyprideis*)

Figure 10

Table 1
List of microfossils and their relative abundance based on a semi-quantitative visual estimation.

Group		Charophytes						Gastropods											Biv.	Ostracods					Fish teeth	Otoliths	Vertebrate teeth
								aquatic									terr.										
Family		Characeae						Melanopsidae	Bithynidae	Hydrobiidae			Valvatidae	Lymnaeidae	Planorbidae	Bithynidae	Carychiidae	Vertiginidae	Strobilopsidae	Sphariidae	Cypricercinae	Cytherideidae	Cypridae	Candonidae				
Sample \ Species		*Nitellopsis (T.) merianii*	*Lychnothamnus barbatus*	*Chara microcera*	*Chara* cf. *globularis*	*Sphaerochara* sp.	*Charaxis* sp.	*Melanopsis buccinoidea*	*Bithynia* sp.	*Semisalsa* sp.	*Islamia* sp.	*Pseudamnicola* sp.	*Valvata saulcyi*	*Radix* sp.	*Gyraulus* cf. *piscinarum*	*Gyraulus* cf. *hebraicus*	*Carychium* sp.	*Vertigo cf. antivertigo*	*Strobilops* sp.	*Pisidium* cf. *moitessierianum*	*Strandesia* sp.	*Cypridеis* sp.	*Cypris pubera*	*Candona* cf. *angulata*			
Section 3	Z-11				•		•				●		•	•	•	•	●	•	•						•		
	Z-10				●	●	•	•			●			•	●			•								•		
	Z-9				•				•		•		•				●			•					•		
	Z-8		•		•			•	●		●		●		●	•	•	•		●		●			•			•
	Z-7				•		•			●	•				•								•		•			
Sect.2	Z-6	•			•			•	●	•	●				•					•			•			•		
	Z-5	•	•		•				•	●	●	●			•					•			•	•		•		
Section 1	Z-4				•		•			●		●																
	Z-3	●			•					●	•	●			•									•				
	Z-2	●	●	●			•		•		●	●			•							•						•
	Z-1	●		●	•				•	●	●	●	•		•	•					•	•						
	Z-0																					•						

Relative abundance (number of specimens per sample) • 1-25 ● 26-100 ● >100

Vertical position of samples represents their relative stratigraphic position, which is indicated in Figs. 6, 7 and 8.